

APPLICATION OF MICROFLUIDICS FOR EMULSION CHARACTERIZATION

By

SUBARNA KOLE

Bachelor of Technology in Chemical Engineering

National Institute of Technology

Raipur, Chhattisgarh (India)

2014

Submitted to the Faculty of the
Graduate College of the
Oklahoma State University
in partial fulfillment of
the requirements for
the Degree of
MASTER OF SCIENCE
July, 2016

APPLICATION OF MICROFLUIDICS FOR
EMULSION CHARACTERIZATION

Thesis Approved:

Dr. Prem Bikkina

Thesis Advisor

Dr. Sundar Madihally

Chair

Dr. Geir Hareland

Member

ACKNOWLEDGEMENTS

I would like to take a moment to thank everyone who supported me during my time at Oklahoma State University and made this thesis possible.

First of all, I would like to thank Dr. Prem Bikkina, my research advisor for his guidance, constant support and providing his expertise and insights in every step of the research work. I also extend my sincere thanks to my committee members, Dr. Sundar Madihally and Dr. Geir Hareland. I would also like to thank Dr. Rob Whiteley, Department Head and Dr. Sundar Madihally, Graduate Program Coordinator for providing me with this wonderful opportunity to carry out research at Oklahoma State University.

Finally, I would like to express my gratitude towards my parents who have encouraged me all these years and have been a constant source of love and support and also to my lab mates and friends who helped me get through difficult times.

Name: SUBARNA KOLE

Date of Degree: JULY, 2016

Title of Study: APPLICATION OF MICROFLUIDICS FOR EMULSION CHARACTERIZATION

Major Field: CHEMICAL ENGINEERING

Abstract: The formation of emulsions is an inevitable process during crude oil production and refining. This emulsion must be separated into its constituent oil and water phases before any further downstream processing. Droplet size is one of the critical factors that influence stability of an emulsion. This thesis focuses on the application of a custom designed microfluidics facility for mono-dispersed oil-in-water (O/W) and water-in-oil (W/O) emulsion formation using hydrophilic and hydrophobic X-junction microfluidic chips, respectively. Water/aqueous salt solutions/aqueous surfactant solutions were used as aqueous phase fluids and n-decane/n-hexadecane/oil soluble surfactant solutions were used as organic phase fluid. The effect of various physical parameters on droplet size and emulsion stability are presented. NaCl, KCl and CaCl₂ salts were used in this study. The type and concentration of these inorganic salts had a negligible effect on the droplet size of both O/W and W/O type emulsions. However, for a given set of external phase and droplet phase velocities, oil droplet size is observed to be considerably larger than the aqueous phase droplets. Oil soluble (Span 80) and water soluble (SDS) surfactants caused a significant reduction in droplet sizes for both O/W and W/O emulsions compared to their respective base case (without surfactant) droplet sizes. Water-cut and oil fraction had no effect on the size of water and oil droplets respectively. Increasing the continuous phase flow rate caused a reduction in the droplet diameter for both O/W and W/O emulsions. N-Decane formed smaller droplets compared to n-hexadecane in O/W emulsions under similar flow rate conditions. It was also observed that the formation of droplets does not necessarily guarantee the stability of emulsions as there can be rapid droplet coalescence in some cases, especially when there is no or low amount of surfactant.

TABLE OF CONTENTS

LIST OF TABLES	vii
LIST OF FIGURES	viii
CHAPTER I.....	10
INTRODUCTION	10
1.1 Emulsions: A Brief Introduction.....	10
1.2 Background of Microfluidics	10
1.3 Motivation for the Research.....	11
CHAPTER II.....	14
REVIEW OF LITERATURE	14
2.1 Emulsions.....	14
2.1.1 Formation.....	14
2.1.2 Classification.....	16
2.1.3 Emulsion Stability.....	17
2.1.4 Current Research on Emulsion Formation and Characterization.....	21
2.2 Physical Phenomena affecting Fluid Flow in a Microchannel.....	22
2.2.1 Capillary Pressure	22
2.2.2 Wettability.....	23
2.2.3 Viscous Forces	23
2.3 Microfluidics.....	24
2.3.1 Common Fabrication Methods.....	25
2.3.2 Emulsion Formation in a MFFD.....	25
2.3.3 Microfluidics Assisted Emulsion Formation and Characterization	25
CHAPTER III	28
METHODOLOGY	28

3.1 Microfluidic System.....	28
3.1.1 Components	28
3.1.1.1 Microfluidic Chip.....	28
3.1.1.2 Pressure pump and flow rate sensors	31
3.1.1.3 Microscope, camera and light source.....	33
3.1.1.4 Tubing, resistors and other accessories.....	34
3.1.2 Chemicals/Reagents	34
3.2 Experimental Procedure.....	34
3.2.1 Setup	35
3.2.2 Emulsion Formation.....	37
3.2.3 Emulsion Stability Analysis.....	38
3.3 Data Analysis.....	38
CHAPTER IV	40
EXPERIMENTAL RESULTS.....	40
4.1 Effect of Various Parameters on Droplet Size	40
4.1.1 Oil and Water fraction/Flow rates.....	40
4.1.2 Organic Phase	44
4.1.3 Salt Type and Concentration.....	45
4.1.4 Surfactant Type and Concentration.....	46
4.2 Stability Analysis	49
CHAPTER V	58
DISCUSSIONS.....	58
5.1 Major Conclusions.....	58
5.2 Future Work.....	59
REFERENCES	61

LIST OF TABLES

Table 1: Classification of surfactants (Farn, 2008).....	20
Table 2: Wetting conditions for water-oil systems (Cassie and Baxter, 1944).....	23
Table 3: Microfluidic Chip Dimensions.....	29
Table 4: Microscope and camera specifications	33

LIST OF FIGURES

Figure 1: Schematic representing emulsification and demulsification process by means of droplet break-up and coalescence (Katepalli, 2014).....	15
Figure 2: Types of emulsions based on the mode of dispersion; (a) W/O emulsion, (b) O/W emulsion, (c) W/O/W emulsion (Kokal, 2005).....	17
Figure 3: Various demulsification mechanisms in an emulsion (Katepalli, 2014).....	19
Figure 4: Fundamental transport processes of surfactant molecules at liquid-liquid interface (Alvarez, 2011)	21
Figure 5: (a) Droplet generation chip (b) Schematic of the chip showing the flow channels (c) Picture of the chip with header (courtesy Dolomite Microfluidics Ltd)	30
Figure 6: Detailed view of the X-junction with droplet generation chip.....	31
Figure 7: Mitos P-pump (Dolomite Ltd).....	32
Figure 8: Flow rate sensor (Dolomite Ltd)	33
Figure 9: Flow diagram of the experimental setup	35
Figure 10: Mitos Flow Control Centre interface	36
Figure 11: Shearing of the droplet phase fluid and droplet formation process.....	37
Figure 12: Continuous stream of n-decane droplets in water are formed at the X-junction of 100 μm hydrophilic chip; continuous phase flow rate = 150 $\mu\text{l}/\text{min}$, droplet phase flow rate = 1.25 $\mu\text{l}/\text{min}$	38
Figure 13: Droplet size measurement using μScope Professional using channel diameter as the reference dimension.....	39
Figure 14: Effect of water-cut on water droplet size; aqueous phase: deionized water; organic phase: n-decane; 100 μm hydrophobic chip	41
Figure 15: Effect of oil% on oil droplet size; aqueous phase: deionized water; organic phase: n-decane; 100 μm hydrophilic chip	42
Figure 16: Effect of oil% on oil droplet size; aqueous phase: 2.5% w/w NaCl solution in water; organic phase: n-decane; 100 μm hydrophilic chip	42
Figure 17: Effect of oil% on oil droplet size; aqueous phase: 12.5% w/w NaCl solution in water; organic phase: n-decane; 100 μm hydrophilic chip	43
Figure 18: Effect of water-cut on water droplet size; aqueous phase: 2.5% w/w NaCl solution in water; organic phase: n-decane; 100 μm hydrophobic chip	43
Figure 19: Effect of water-cut on water droplet size; aqueous phase: 12.5% w/w NaCl solution in water; organic phase: n-decane; 100 μm hydrophobic chip	44

Figure 20: Effect of organic phase on oil droplet size; continuous phase: DI water; droplet phase flow rate = 0.75 $\mu\text{l}/\text{min}$; 100 μm hydrophilic chip	45
Figure 21: Effect of salt concentration and salt type on oil (in hydrophilic chip) and water (in hydrophobic chip) droplet size; droplet phase flow rate = 0.75 $\mu\text{l}/\text{min}$, continuous phase flow rate = 150 $\mu\text{l}/\text{min}$	46
Figure 22: Effect of SDS concentration on oil and water droplet size, continuous phase flow rate = 150 $\mu\text{l}/\text{min}$, droplet phase flow rate = 0.75 $\mu\text{l}/\text{min}$; 100 μm chip	47
Figure 23: Effect of Span 80 concentration on oil and water droplet size, continuous phase flow rate = 150 $\mu\text{l}/\text{min}$, droplet phase flow rate = 0.75 $\mu\text{l}/\text{min}$; 100 μm chip	48
Figure 24: Effect of SDS concentration on oil and water droplet size, continuous phase flow rate = 200 $\mu\text{l}/\text{min}$, droplet phase flow rate = 0.75 $\mu\text{l}/\text{min}$; 100 μm chip	48
Figure 25: Effect of Span 80 concentration on oil and water droplet size, continuous phase flow rate = 200 $\mu\text{l}/\text{min}$, droplet phase flow rate = 0.75 $\mu\text{l}/\text{min}$; 100 μm chip	49
Figure 26: Stability analysis for O/W emulsion; aqueous phase: deionized water, oil phase: n-decane; (a) immediately after emulsion formation, (b) after 8 hours.....	51
Figure 27: Stability analysis for O/W emulsion; aqueous phase: deionized water, oil phase: 2.5 g/l Span 80 solution in n-decane; (a) immediately after emulsion formation, (b) after 8 hours	53
Figure 28: Stability analysis for O/W emulsion; aqueous phase: 0.5 g/l SDS solution in water, oil phase: n-decane; (a) immediately after emulsion formation, (b) after 8 hours. 55	
Figure 29: Stability analysis for O/W emulsion; aqueous phase: 2.5 g/l SDS solution in water, oil phase: n-decane; (a) immediately after emulsion formation, (b) after 8 hours. 57	

CHAPTER I

INTRODUCTION

1.1 Emulsions: A Brief Introduction

Emulsions are known for their widespread use in our daily life. Due to this they have generated a great practical interest. Some common examples of emulsions that we encounter on a regular basis are those occurring in food, pharmaceuticals, cosmetics and agricultural products [1-3]. Apart from these emulsions are also encountered in almost every stage of petroleum recovery process [4].

Crude oil is composed of a range of hydrocarbons (alkanes, naphthenes and aromatic components), phenols, carboxylic acids, water and metals. It also consists of significant amount of sulfur and nitrogen compounds. Due to this, there is a tendency for the formation of various types of stable and unstable emulsions in the crude oil [5].

1.2 Background of Microfluidics

Stability of emulsions depends on a number of factors, droplet size being one of the most important. Composition of the phases and water-cut/oil fraction are also critical factors that determine the stability of emulsions. A systematic study of all these properties can lead to a better understanding of emulsification and demulsification processes. There are a number of methods that can be used to create and characterize them. Microfluidics provides a convenient way to study emulsion formation and stability. The field of microfluidics has been popularized in the last 2-3 decades since the term “miniaturized total analysis system (μ TAS)” was coined by Andreas Manz [6]. In general,

a microfluidic device refers to a chip usually made of a transparent material with etchings on the surface for the flow of fluids. Two such substrates containing etchings are sealed together to create a closed channel [7]. As the dimensions of a system decrease the surface phenomena become more and more dominant and pressure gradients, surface tension effects and capillary forces dictate the behavior of the system. For example, in a microfluidic device, the motion of fluids can be significantly influenced by changing surface tension of liquid-liquid/gas-liquid interface and altering the wettability of surfaces involved [8]. Microfluidics offers numerous research possibilities in the field of medicine, electronics, chemical and energy industries.

1.3 Motivation for the Research

Production of oil involves its movement through porous rocks and fractures in limestone, sandstone and other minerals. It is observed that the characteristic length-scale associated with the pores in these rocks and minerals are in the micro-scale level. At these length-scales the phenomena of capillary effects, viscous forces and interfacial tension become dominant, overcoming the effects of gravity. Therefore, the use of microfluidic devices can help us to get a basic understanding of the critical factors that govern the extraction of oil [9]. Although, a lot of work has been carried out to analyze emulsification and demulsification kinetics in crude oil mixtures, the area of microfluidics based emulsion formation and stability and its application in enhanced oil recovery is still in its early phase. Some common areas where microfluidics has been used for enhanced oil recovery (EOR) studies include polymer, surfactant, foam, and nanoparticle floodings, microbial EOR, and heavy oil extraction. Flooding simply refers to the displacement of oil in a reservoir by pushing it with a displacing fluid. Dupas et al. (2012) performed a study to investigate the effect of mechanical extension of polymer chains on the efficiency of flooding process. The polymer samples were tested for extensional properties using a microfluidic device EVROC (Extensional Viscometer and Rheometer on-a-chip) [10]. Surfactant and water flooding are also common areas of interest in microfluidics. He et al. (2014) compared the effects of weak emulsifying surfactant

(WES) and non-emulsifying surfactant (NES) for oil production from shale. The Reservoir-on-a-chip (ROC) device used by them consisted of a random porous network within a cross-sectional area of $400 \times 600 \mu\text{m}^2$. The pore sizes in the chip were consistent to that of shale formations. Results of that study clearly indicated that WES yielded higher oil recovery compared to NES fluids [11]. Nanoparticle (NP) based EOR studies were conducted by Xu et al. (2015) in which a microfluidic chip with T-junction was used to create monodispersed droplets of oil in water and nanoparticles were present in the aqueous phase. Increase in NP concentration decreased oil droplet size which means an easier oil recovery process in actual reservoir [12]. The reason behind effect of NP on oil recovery is not very well understood and it is attributed to reduction in interfacial tension (IFT), viscosity and wettability alteration. However, the dominant mechanism is still not clear. Foam flooding is a process to extract oil preferably used due to its high viscosity. Conn et al. (2014) used two microfluidic devices, first device to pre-generate foam and the second device to study the effect of foam flooding on oil displacement. The presence of bubbles in foam caused a high pressure drop and higher apparent viscosity which led to effective displacement of oil from low permeability zones. In fact, foam flooding was found to be more effective than water, gas and surfactant floodings themselves under similar conditions [13]. A micromodel designed by Wildenschild et al. (2012) was used to find out the effectiveness of Microbial Enhanced Oil Recovery (MEOR) based on capillary number and wettability of micro-channels [14]. EOR methods for heavy oil extraction are quite challenging due to unfavorable mobility ratios between aqueous and oil phases. Dong and co-workers (2012) discussed an alkaline flooding technique for heavy oil extraction. A strongly water-wet glass micromodel was used and it was demonstrated that alkaline solution (a mixture of NaOH and Na_2CO_3 solution) could significantly improve sweep efficiency and oil recovery [15]. In spite of all these studies, at present the use of microfluidics has not reached a point where it can significantly influence oil recovery techniques.

There are a number of reasons as to why the use of microfluidics is not more widespread given its potential in the oil and gas industry. The production of micro-models that mimic actual formations is still a big challenge. The process involved in field trials of the microfluidic models can be very expensive as well as time consuming [16]. With the advent of new technology, more avenues of research in this field are opening up. In his review paper, Lifton (2016) discussed several future possibilities for the use of microfluidics in oil production for example liquid front control within curved or bent channels, hydraulic fractures and modification of surface properties of reservoir walls. 3D printing of microfluidic chips directly from a CAD software input file is a promising method for rapid prototyping of micromodels [16].

This thesis focuses on the use of microfluidic chips to generate monodispersed water-in-oil (W/O) and oil-in-water (O/W) emulsions. Hydrophilic chips were used to create O/W emulsions while hydrophobic chips were used to create W/O emulsions. N-decane/n-hexadecane/Span 80 solution in n-decane is used as the oil phase fluid. Deionized water/solution of sodium dodecyl sulfate (SDS) solution in water/inorganic salt solutions in water is used as the aqueous phase. A detailed parametric study is carried out to find out the effects of various process variables on the droplet size. Stability experiments were also carried out and they give us an idea of droplet-droplet and droplet-interface coalescence phenomena with and without the presence of surfactants. This work can be useful to get an idea of underlying concepts that govern fluid flow in the length-scales encountered in reservoirs as well as the factors affecting emulsion formation and stability of crude oil emulsions. The major applications include study of Enhanced Oil Recovery (EOR) by creating emulsions and foams, sweep efficiencies for different permeability zones based on droplet size of emulsions, and obtain relative permeability curve based on this data.

CHAPTER II

REVIEW OF LITERATURE

2.1 Emulsions

The International Union for Pure and Applied Chemistry (IUPAC) defines emulsion as a fluid system in which droplets of one liquid are dispersed in another liquid [17]. The general name for any system containing two phases is called a colloid. When both phases are liquids, the term emulsion is used.

2.1.1 Formation

An emulsion is created when two immiscible liquids, typically oil and water are mixed together to form droplets of one liquid in the other liquid. It consists of two phases: the droplet or dispersed phase and the continuous phase [18]. Although they appear to be homogeneous at a macroscopic level, emulsions are usually heterogeneous at microscopic level. The process of creating an emulsion by mixing together two liquids is called emulsification. Figure 1 represents a schematic of emulsification and demulsification processes involving droplet break-down and coalescence.

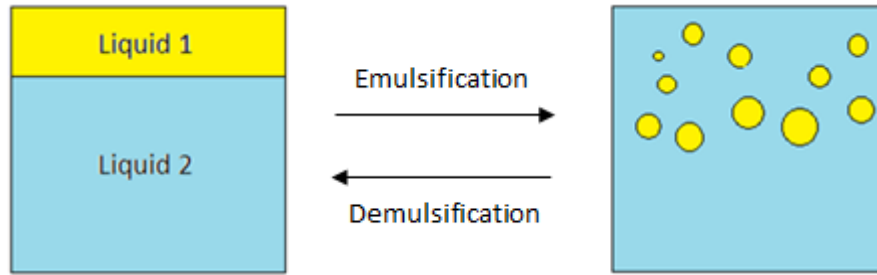


Figure 1: Schematic representing emulsification and demulsification process by means of droplet break-up and coalescence (Katepalli, 2014)

There are a number of methods outlined in the literature for creating an emulsion. Each one of them offers certain advantages and disadvantages. Conventionally, mechanical devices such as high speed blenders, high pressure valve homogenizers, and colloid mills are used to form small droplets. However, it may also be possible to use low energy methods for emulsion formation in certain systems where spontaneous formation of droplets takes place on mixing of two liquids [19].

McClements et al. (2006) used high-speed blender (M133/1281-0, Biospec Products, Inc., ESGC, Switzerland) to produce primary emulsion by mixing 5 wt% corn oil with a 95 wt% emulsifier solution followed by two passes through a two stage high-pressure valve homogenizer (LAB 1000, APV-Gaulin, Wilmington, MA). The primary emulsion was mixed with chitosan solution to produce a secondary emulsion. The mixture was homogenized by stirring with a magnetic stirrer for an hour. Finally, tertiary emulsions were formed by diluting the secondary emulsion with aqueous pectin solutions to form series of emulsions containing varying concentrations of pectin [20].

It is also possible to generate nano-emulsions using high shear stirring, high pressure homogenizers and ultrasound generators [21]. These equipment are capable of supplying high amounts of energy in a very short time, essential for creating these emulsions. The operating pressure conditions for a high pressure homogenizer usually ranges from 50-100 MPa although pressures as high as 350

MPa have been achieved in some recently developed instruments. Ultrasonic emulsification is also an effective method to generate small droplets. However, it is suitable for small batches only [22].

2.1.2 Classification

Based on the size of droplets, emulsions can be distinguished into three categories: 1) Macroemulsions, with droplets > 400 nm, 2) Miniemulsions, with droplets between 100 and 400 nm and 3) Microemulsions, with droplets < 100 nm. Another way to classify emulsions is based on droplet and continuous phases: 1) O/W type emulsions, 2) W/O type emulsions and 3) multiple emulsions that can be oil-in-water-in-oil (O/W/O) type or oil-in-water-in-water (W/O/W) type [23]. Figure 2 shows the various types of emulsions based on which phase is dispersed and which phase is continuous; (a) water droplets dispersed in a continuous oil phase, (b) oil droplets dispersed in a continuous aqueous phase (c) W/O/W (multiple) emulsion with small droplets of water dispersed in bigger oil droplets which are, in turn, dispersed in a continuous water phase.

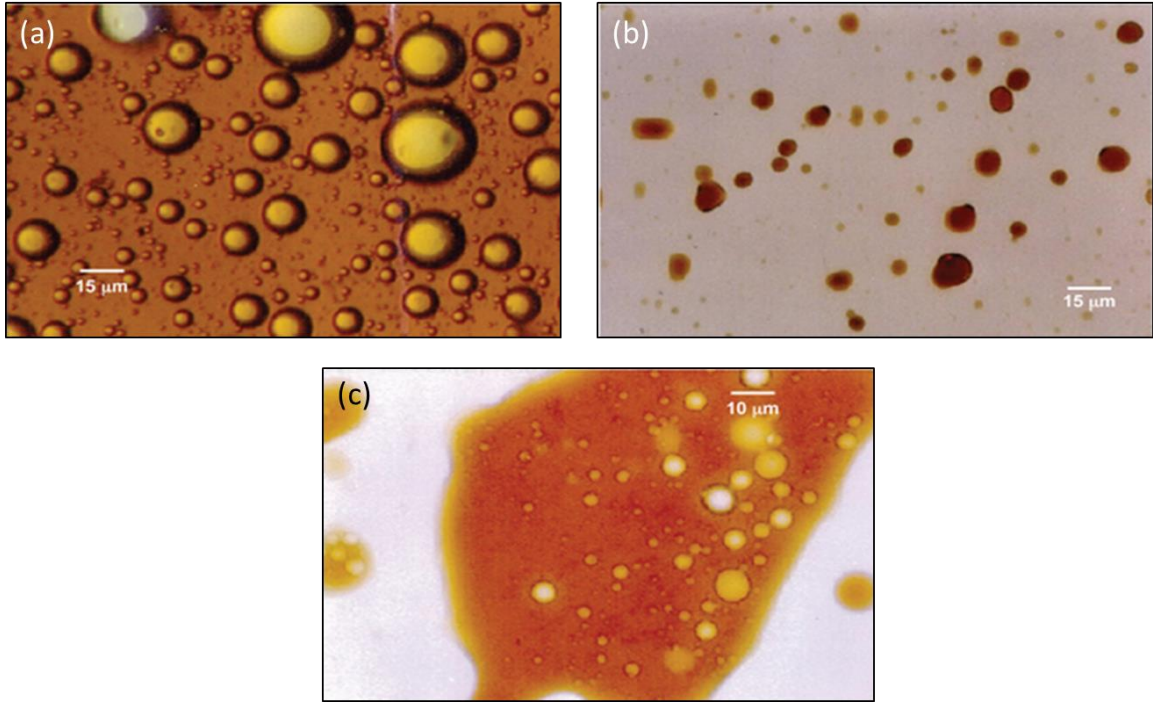


Figure 2: Types of emulsions based on the mode of dispersion; (a) W/O emulsion, (b) O/W emulsion, (c) W/O/W emulsion (Kokal, 2005)

2.1.3 Emulsion Stability

Significant amount of energy is required to make an emulsion. In order to break a droplet in an emulsion into smaller droplets, first it has to be deformed. For a curved surface the difference in pressure between convex and concave interface, also known as the Laplace pressure, is expressed by [24]

$$p_L = \gamma \left(\frac{1}{R_1} + \frac{1}{R_2} \right) \quad (1)$$

where, γ is the interfacial tension and R_1 and R_2 are the principal radii of curvature.

In case of a spherical droplet of radius r it reduces to $2\gamma/r$. It means that to deform a water drop of radius 1 micron, a Laplace pressure of 2000 Pa has to be applied which is a significant amount pressure over a very small distance of the order of 1 micrometer [24]. This energy can be applied

using high speed blenders or homogenizers as discussed in the last section or by shear stress induced due to velocity gradient or pressure difference within the fluid.

The final droplet distribution within the emulsion is governed by two competing processes: 1) droplet break-up and 2) droplet coalescence (droplet-droplet and/or droplet-interface coalescence). In a flow induced coalesce process, when two droplets approach each other, initially they slide past one another. At this point the line connecting the center of these droplets is no longer parallel to the flow path. There is a thin film of continuous phase between these droplets that drains away over time. Drainage of this film is promoted by the excess capillary pressure while the viscous stress reduces the rate of drainage. Hence the ratio of viscous stresses to the capillary forces is an important parameter governing droplet coalescence [25]. It is defined by the Capillary number (Ca) and expressed as

$$Ca = \mu V / \gamma \quad (2)$$

where, μ is the dynamic viscosity of the continuous phase, V is the velocity of continuous phase and γ is the interfacial tension between the phases.

In most cases when oil and water are mixed with each other, they tend to separate almost instantaneously containing two separate layers of oil and water. This is because formation of droplets increases the overall energy of the system since there is an increase in oil-water interfacial area. Figure 3 highlights the major demulsification mechanisms in an emulsion i.e. Ostwald ripening, aggregation, sedimentation and coalescence. While mixing two immiscible liquids, they tend to form two separate layers which can be avoided by using a stabilizing agent (emulsifier or surfactant). The role of a surfactant is to prevent the merging or coalescence of droplets with each other. Surfactant is a contraction of the term surface active agent and refers to a substance that has the property of getting adsorbed at the interface of a system. In this process, it alters the interfacial energy of the system which is defined as the minimum amount of work required to create the interface [26, 27].

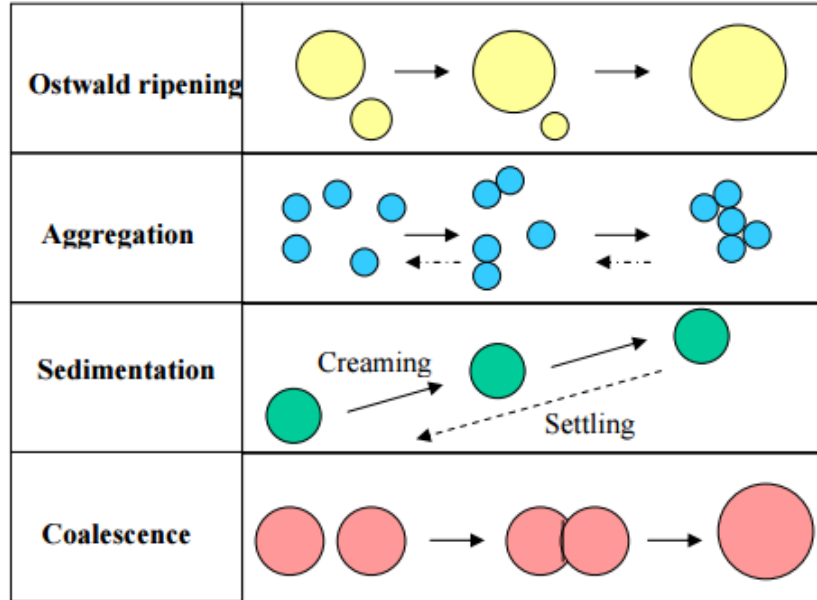


Figure 3: Various demulsification mechanisms in an emulsion (Katepalli, 2014)

Surfactants are basically organic compounds consisting both lyophilic (solvent-loving) as well as lyophobic (solvent-fearing) groups in their molecule. In the particular case when water is used as the solvent the terms are referred to as hydrophilic and hydrophobic, respectively. When a surfactant is added to solvent, two processes take place: adsorption and aggregation. Adsorption is the process of migration of surfactant molecules to the liquid-liquid/gas-liquid interface to orient themselves in a way that minimizes interaction between the hydrophobic part and water molecule. Clusters of surfactant molecules may also form within the solution in such a way that the hydrophilic groups are oriented towards the aqueous phase. This process is called aggregation or micellization and the aggregates are known as micelles. Micelle formation starts when concentration of surfactant reaches a value known as Critical Micelle Concentration (CMC). Surfactants can be either anionic, cationic, non-ionic, or amphoteric [26, 27].

Table 1: Classification of surfactants (Farn, 2008)

Type of surfactant	Characteristics
Anionic	Dissociate in water to form both negatively and positively charged ions, the hydrophilic head is negatively charged
Cationic	Also dissociate to form both negatively and positively charged ions but the hydrophilic head is positively charged
Non-ionic	Do not dissociate in water, commonly used as emulsifiers
Amphoteric	Can have positive or negative charge on the hydrophilic head depending on pH, exist as zwitterions in an intermediate pH

A surfactant (emulsifier) reduces the interfacial tension between the two phases present that increases the stability of emulsion. It also creates a steric or electrostatic repulsion that prevents coalescence among individual droplets. According to the Bancroft's rule surfactant should be chosen in such a way that it is soluble in the continuous phase to a higher extent as compared to the droplet phase [27]. Figure 4 below shows the fundamental transport processes of surfactant molecules at liquid-liquid interface. The surfactant molecules that are present near the interface are constantly undergoing adsorption and desorption phenomena from bulk of the continuous phase fluid to the interface. A concentration gradient also gives rise to diffusion of surfactant from bulk to the interface.

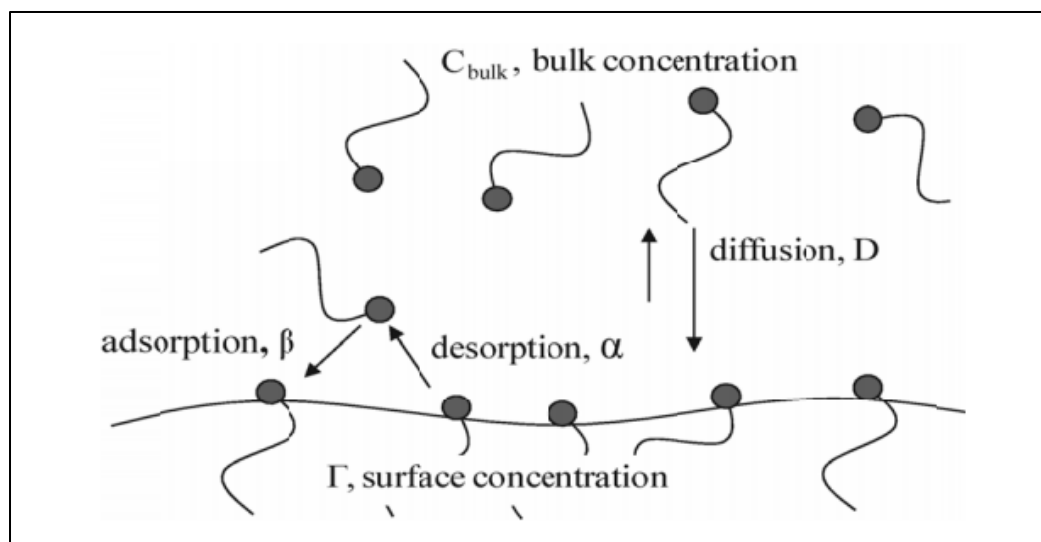


Figure 4: Fundamental transport processes of surfactant molecules at liquid-liquid interface (Alvarez, 2011)

2.1.4 Current Research on Emulsion Formation and Characterization

Emulsion formation can be a favorable process in many cases but often it can be undesirable as well. They are often encountered in crude oil production in the form of W/O type emulsions. In order to successfully mitigate the problems related to emulsification, a proper understanding of the emulsion behavior, stability and characteristics under various conditions is important. Hence, characterization of emulsions is the first step in the destabilization/demulsification process. To study the emulsification and demulsification kinetics, emulsions have been prepared in laboratory by various researchers to simulate the crude oil obtained from an oil well. Usually a known amount of water/brine solution is added to the oil phase while the mixture is being hand-shaken followed by rapid mixing in a homogenizer. Standard laboratory stirrers may also be employed fitted with an impeller blade to stir the liquid. For a given emulsion, average droplet size can be controlled by varying the stirring speed and time. Characterization of emulsion involves determining the droplet size distribution and water content. Karl-Fisher reagent method can be used to determine the water content of an emulsion in accordance with ASTM D-1744 procedures. Karl-Fisher reagent contains

iodine which selectively reacts with water present in the emulsion. The emulsion initially conducts electricity in a titration cell in the absence of reagent. The amount of reagent needed to make the emulsion non-conductive determines its water content [28]. In an experiment conducted by Fortuny et al. (2008) the Malvern Instrument Model 2000 Mastersizer particle-size analyzer was used to find out the droplet size distribution, the working principle of which is based on the laser diffraction technique. The detection range of the instrument varied from 0.020 to 2000 μm [29]. McClements and Coupland (1996) have explained a detailed procedure to determine droplet size distribution using ultrasonic spectroscopy in their research paper [30]. FTIR (Fourier Transform IR) spectra in combination with a gas chromatograph is a common method to determine the analytical properties of emulsions [31].

2.2 Physical Phenomena affecting Fluid Flow in a Microchannel

The flow of a fluid in microchannels is governed by various physical phenomena that affect stability, droplet size and type of emulsion formed. The effect of most important phenomena are discussed in the subsequent sections.

2.2.1 Capillary Pressure

Capillary pressure can be defined as the difference in pressure between the two immiscible fluids at the interface. When the fluids flow through a channel, pressure is higher in the non-wetting phase. Therefore, it is the difference in pressure of non-wetting phase and the wetting phase [32]. In a typical reservoir, capillary forces depend on the geometry, pore size, wettability, and interfacial properties of the rock and fluids [33]. Emulsions that are stabilized by solid particles are called as Pickering emulsions and the stability of the emulsion depends on the capillary force between the solid particles at the oil-water interface [34].

2.2.2 Wettability

One common method to characterize porous rock wettability is based on whether it is preferentially water-wetting or oil-wetting. In some cases, neutral wettability is also used as a third classification [35]. A solid surface is considered oil-wet if it shows an oil advancing contact angle less than 90° when measured through the oil side at the oil-water interface. In such a system oil will displace water if both are supplied at same pressure. A similar definition is applicable for water-wet surface [35]. The wetting conditions for water-oil system are mentioned in Table 2 below.

Table 2: Wetting conditions for water-oil systems (Cassie and Baxter, 1944)

Wetting condition	Contact angle (degrees)
Strongly water-wet	0-30
Moderate water-wet	30-75
Neutrally wet	75-105
Moderately oil-wet	105-150
Strongly oil-wet	150-180

2.2.3 Viscous Forces

Viscosity results in pressure drop of fluid flowing through a porous medium or a microchannel. Flow of fluid in the medium depends on the magnitudes of viscous and capillary forces. In order for the fluid to flow the viscous forces must be larger than the capillary forces. If a porous medium is considered as a bundle of capillary tubes, then the pressure drop in each one of these capillaries in a laminar flow can be given by [32]

$$\Delta P = \frac{8\mu L v_{avg}}{r^2 g_c} \quad (3)$$

where,

ΔP = pressure difference across capillary tube

μ = viscosity

L = length of capillary tube

v_{avg} = average velocity of fluid in the capillary tube

r = radius of capillary tube

g_c = gravitational constant

The viscous forces for fluid flow in porous media is given by Darcy's law [27].

$$\nabla P_v = -\frac{\mu u_s}{K} \quad (4)$$

where,

∇P_v = pressure gradient due to viscous forces

μ = dynamic viscosity of the fluid

u_s = superficial velocity of the fluid

K = permeability of the porous medium

2.3 Microfluidics

Microfluidics is an emerging field with increasing applications over the last few years. It is the field of science and technology dealing with extremely small amounts of fluids (order of 10^{-9} to 10^{-18} liters) [36]. To consider the system as a microfluidic at least one dimension of the channels should be in the order of micrometer or tens of micrometers. It provides a convenient method for producing emulsions, study their stability and other characteristics. The major advantages of using microfluidic devices are precise control of droplet size by adjusting the flow rates of fluids, ease in scaling up and absence of turbulence allowing easy modelling of flow and transport.

A microfluidic flow-focusing device (MFFD) is used for the generation of emulsions.

2.3.1 Common Fabrication Methods

The materials used for fabrication of microfluidic devices has greatly evolved in the last two decades. Glass or quartz are often known as the first generation materials and they have been used for this purpose even before the concept of microfluidics was introduced. Photolithography is employed to create a micro pattern on a glass wafer and the channels are sealed by using a substrate through fusion bonding process [37]. Elastomers and plastics are an inexpensive alternate to glass and quartz. They provide the flexibility of choosing a range of materials based on their specific property. PDMS (polydimethylsiloxane) is the most widely used elastomer for microfluidic applications due to its convenience in fabrication and high elasticity [36]. Thermosets and thermoplastics can also be used for fabricating microfluidic chips depending on the application and economic considerations [38].

2.3.2 Emulsion Formation in a MFFD

Microfluidic flow focusing devices usually consist of an X or a T-junction to produce monodispersed droplets by shearing of the droplet phase fluid by a continuous phase fluid. In case of X-junction, there are two continuous phase inlets and a droplet phase inlet. An outlet is provided for the flow of emulsion. It provides a convenient method for producing emulsions and to study their formation and characteristics.

2.3.3 Microfluidics Assisted Emulsion Formation and Characterization

Microfluidic chips can be used to form monodispersed O/W and W/O emulsions for a number of applications including food industry, chemical reactions, cell culture to name a few. A number of food products are essentially dispersions or foams of O/W or W/O. Microfluidic devices can be used to control the size and concentration of the phases in the emulsion and tailor certain properties of the product. The fast mixing of reagents in food industries can also be achieved in a microfluidic

flow focusing device [39]. It is also useful for carrying out controlled chemical reactions. Compartmentalization of reactions in droplets is possible by using microfluidics. Major applications include acceleration of various chemical and biochemical reactions, protein crystallization and study of enzyme characteristics [40].

Microfluidics has several applications in Oil Recovery Processes also. During the production of oil, it has to travel through porous rock and other restrictions in the wellbore and flow lines. The fluid obtained from the well contains significant amount of water apart from crude oil and this water has to be separated before any further downstream processing [41]. This fluid is typically a W/O type emulsion. As the mixture is separated during several stages, concentration of water increases to a point where the fluid inverts into an O/W emulsion. Further, with an increase in production time the oil content in the given field will reduce which also leads to the production of O/W emulsion from the oil well. Various methods are employed in order to separate this mixture including mechanical devices like gravity settlers, or centrifugal separators such as hydrocyclones. Separation is enhanced if droplets in the mixture coalesce with each other. In order for this to work the time scale of coalescence should be smaller than the residence time of fluids in the separator. The coalescence of droplets depends on a lot of different factors like nature of flow, physical properties of fluids, presence of surfactants or demulsifying agents in the emulsion. A convenient way to examine droplet coalescence in an emulsion is through the use of a microfluidic flow focusing device. Numerous studies have been carried out to address droplet coalescence in microfluidic devices. In most of these studies n-hexadecane and n-decane (with or without appropriate surfactants) are used as the organic phase fluid to emulate certain properties of crude oil like viscosity and interfacial tension between crude oil water. The aqueous phase liquid can be deionized water, or an aqueous solution of salt and/or surfactant. These devices can be fabricated to simulate the flow conditions which are encountered in the oil field. Microfluidics can also be used for the creation of foam for studying foam flooding in Enhanced Oil Recovery (EOR) process.

It involves the formation of bubbles in a microchannel. The process of creating foams is similar to that of creating an emulsion. Gas phase flows through a tiny orifice and sheared into small bubbles by a liquid jet. This is known as the flow focusing method [42]. So, it has a potential to serve as an important tool to predict water-crude oil demulsification kinetics and assist in the study of oil recovery process [43].

CHAPTER III

METHODOLOGY

3.1 Microfluidic System

The microfluidic system used for this study consists of a droplet generator chip, pressure pumps, flow rate sensors, flow resistors, microscope, camera and light source to generate highly monodispersed droplets in a continuous phase. The size of droplets produced by 100 μm chip typically ranges from 30-150 μm in diameter. All the components are described in detail below:

3.1.1 Components

3.1.1.1 Microfluidic Chip

The most important component of the experimental setup is the microfluidic chip supplied by Dolomite Microfluidics Ltd. It is a microfluidic device containing channels for the flow of continuous and dispersed phase fluids. It consists of two types of junctions: X-junction and T-junction on a single chip. In this thesis, the X-junction has been used exclusively for droplet generation and emulsion formation. As shown in figure 5, there are two inlets for the continuous phase fluid and one inlet for droplet phase fluid and an outlet for the flow of emulsion. Both of these fluids interact at the junction where a stream of dispersed phase fluid is converted to droplets due to the shear stress of continuous phase fluid.

The microfluidic chip was fabricated by Dolomite Microfluidics Ltd, from glass using Hydrofluoric

acid (HF) etching and thermal bonding. A buffered solution of HF was used for etching process while thermal bonding involves heating the glass substrates to their glass transition temperatures and application of high pressure resulting in very high bond strength comparable to cohesive forces in the bulk material.

Specifications of the hydrophobic and hydrophilic chips used in this study are outlined below:

Table 3: Microfluidic Chip Dimensions

Channel cross-section at junction (depth x width)	100 μm x 105 μm
Wide channel cross-section (depth x width)	100 μm x 300 μm
Channel length after junction	11.25 mm
Volume of channel after junction	0.31 μl
Back pressure with 100 $\mu\text{l}/\text{min}$ flow of water	0.0002 Bar
Surface roughness of channels	5 nm
Chip size (length width x thickness)	22.5 mm x 15.0 mm x 4 mm
Maximum operating pressure	30 Bar

Two types of chips were used: hydrophilic and hydrophobic channels. The hydrophilic droplet junction chip was used to create O/W emulsions while the one with hydrophobic coating was used to produce W/O type emulsions. The chip is fitted with a header for making connections to pumps via tubing.

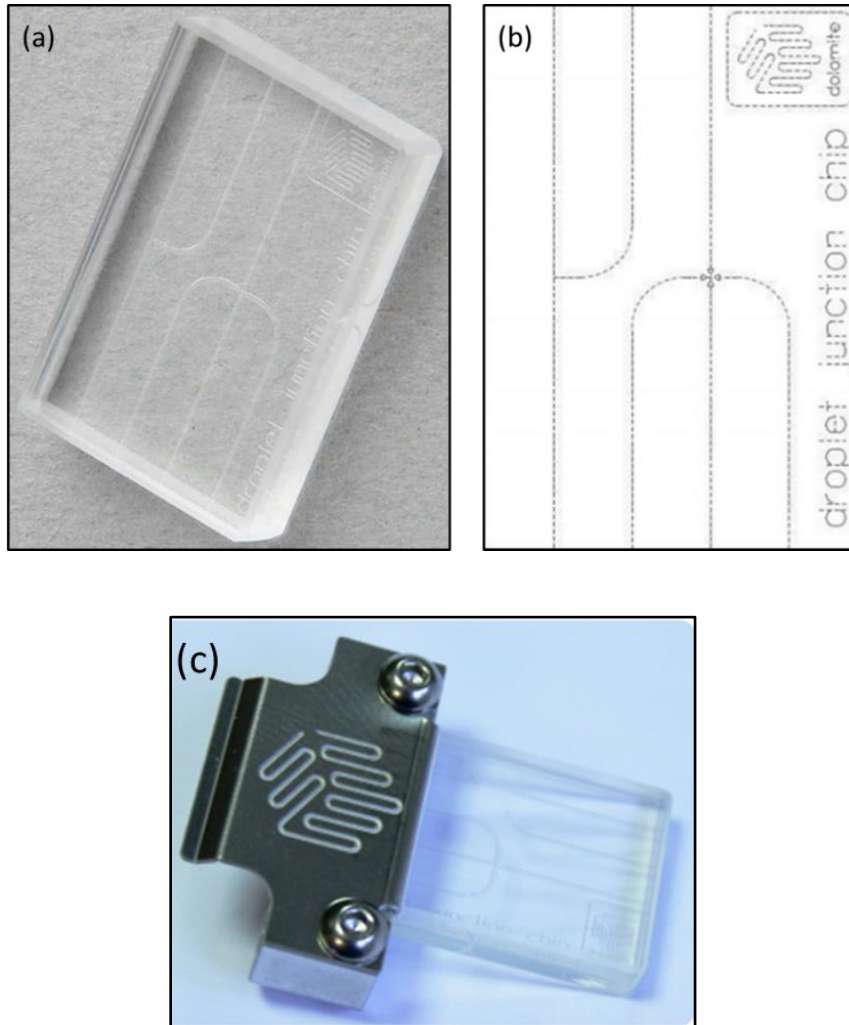


Figure 5: (a) Droplet generation chip (b) Schematic of the chip showing the flow channels (c) Picture of the chip with header (courtesy Dolomite Microfluidics Ltd)

Figure 6 shows a detailed view of the X-junction in the chip with a continuous monodispersed stream of droplets.

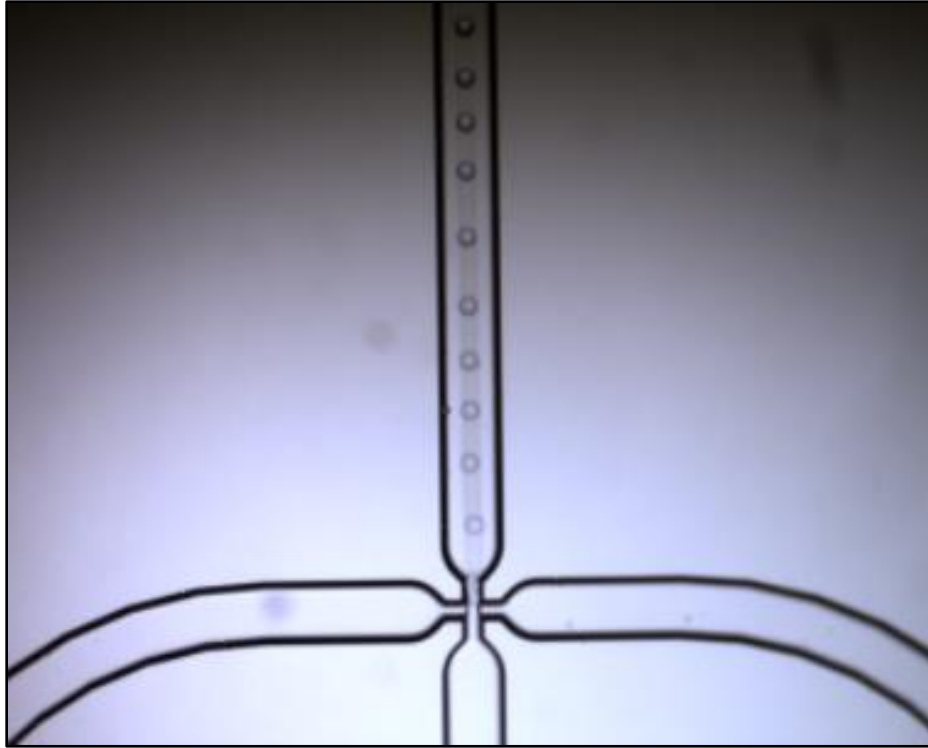


Figure 6: Detailed view of the X-junction with droplet generation chip

3.1.1.2 Pressure pump and flow rate sensors

Two Mitos P-pumps as shown in figure 7 were used to transport the continuous and droplet phase fluids to the microfluidic chip. A continuous supply of filtered, desiccated air provides the required pressure needed to circulate the fluids. The pumps can operate at pressures up to 10 Bar.

For better control and accuracy of flow rates a closed loop control is used which essentially means that the pumps are connected to flow rate sensors by means of a sensor interface. They are connected to a computer via RS232 serial interface which allows us to control the flow rate or pressure. It is extremely useful to provide a pulseless liquid flow especially suitable for microfluidic applications. The main advantages are precise control of flow control, wide range of operating pressure, fast response time and excellent chemical resistance [Dolomite microfluidics Ltd].

Flow sensors (figure 8) with a wide range of flow rates can be used with the pumps depending on

the volume fraction of the phases in the emulsion. In this case, a 30-1000 $\mu\text{l}/\text{min}$ MitoS flow rate sensor was used for continuous phase fluid and 0.07-1.5 $\mu\text{l}/\text{min}$ MitoS flow rate sensor was used for the droplet phase fluid. The flow rate sensors consist of a highly sensitive microsensor chip which is isolated from the flow media by channel walls made of glass, ceramic or plastic. A heating element on the chip adds minimal amount of heat to the medium and two temperature sensors located symmetrically upstream and downstream of the heat source detect the temperature changes. This provides information about the heat transfer rate which is directly related to flow rate of the liquid.



Figure 7: MitoS P-pump (Dolomite Ltd)



Figure 8: Flow rate sensor (Dolomite Ltd)

3.1.1.3 Microscope, camera and light source

An integrated system of a high speed microscope (Nikon stereoscopic zoom SMZ745T) and a CCD (Charge Coupled Device) camera (PixeLINK B742) was used to capture high quality images and videos of droplet formation process. A 15V/150W illuminator (Schott KL 1600 compact) was used to provide illumination with the help of a fiber optic light guide.

The specifications of the microscope and camera are given below:

Table 4: Microscope and camera specifications

Component	Specifications
Microscope	7.5x zoom range 6.7x-50x magnification 115 mm working distance 3.5-25 mm field of view
Camera	1.3 megapixel (1280x1024) 1000 frames per second (fps) 0.04 ms -1s exposure time

3.1.1.4 Tubing, resistors and other accessories

The tubing used to connect pumps and flow sensors to the chip are made of FEP (Fluorinated ethylene propylene). They have 250 μm inner diameter (ID) and 1/16" outer diameter (OD) while the flow resistors are 100 μm ID and 1/16" OD tubing. An ETFE (ethene-co-tetrafluoroethene) T-connector was used to divert the flow from the continuous phase pump to two different inlets of the chip. All these components were chosen to be chemically compatible to water and organic phase liquids used in these experiments.

3.1.2 Chemicals/Reagents

To produce O/W and W/O emulsions, deionized water, aqueous salt solutions, or solution of Sodium Dodecyl Sulfate (SDS) in water or brine are used as aqueous phase. N-decane, n-hexadecane or a solution of Span 80 in n-decane is used as the organic phase fluid. The salts used were Sodium Chloride (> 99.0%) obtained from Alfa Aesar, Potassium Chloride (ACS Grade) and Calcium Chloride (ACS Grade) both supplied by Amresco Inc. N-decane (> 99.0%) was supplied by TCI and n-hexadecane (99%) by Alfa Aesar. Isopropanol (99%), which is used as a cleaning fluid for the chips and tubing was obtained from Pharmaco-Aaper. Span 80 (> 99.0%) was supplied by TCI and ultra-pure SDS was obtained from MP Biomedicals, LLC.

3.2 Experimental Procedure

All the components were assembled to obtain a microfluidic setup, shown in figure 9, that was used for this research. The data obtained from the setup was analyzed and the effects of various process parameters on droplet size and emulsion stability was investigated.

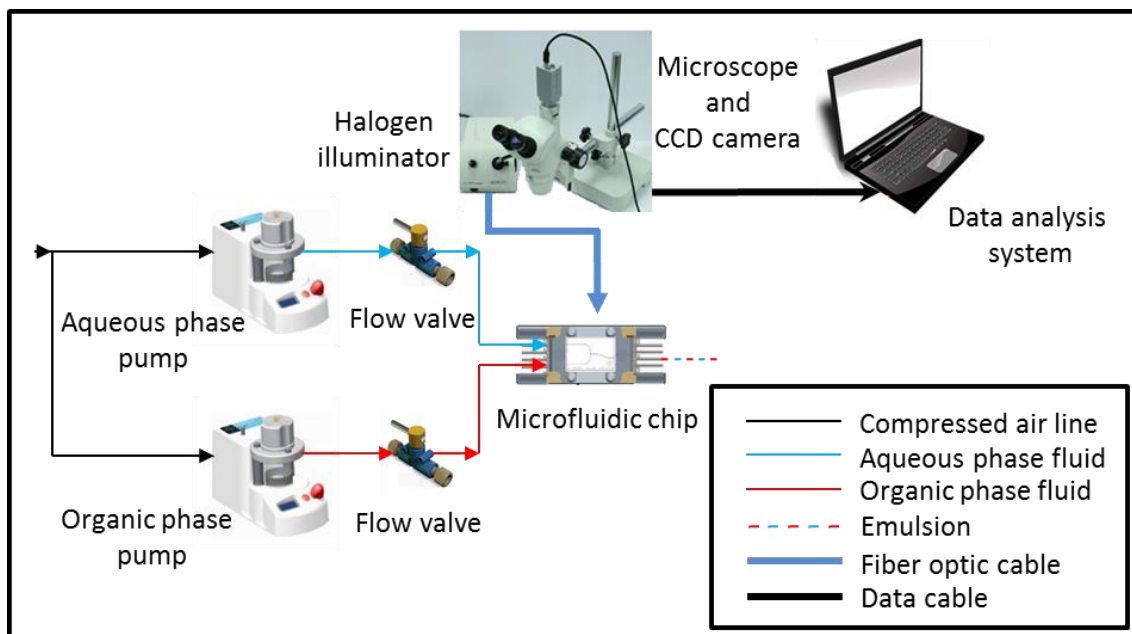


Figure 9: Flow diagram of the experimental setup

3.2.1 Setup

First of all, both the pumps were connected to a compressed air source supply using a T-connector. After that, the flow rate sensors were attached to the pumps using the sensor interfaces. Mitos Flow Control Center Software (FCC version 2.5.15) was installed on the desktop. The pumps were connected to PC using USB to RS232 Adaptor Cable. Next, power cables for the pumps were plugged into a power outlet. The aqueous and organic phase fluids were filled in glass vials and placed inside the respective pump chambers on a holder. Once this was done the FCC detects the pumps and flow rate sensors as shown in figure 10.

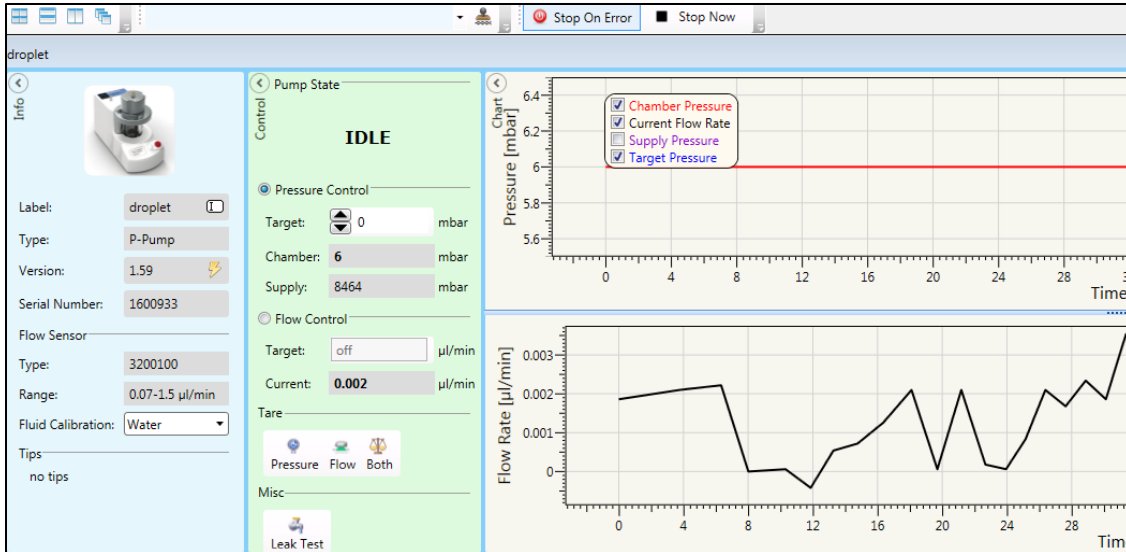


Figure 10: Mitos Flow Control Centre interface

The next step was setting up the camera and microscope system. The microscope stand was placed on a level surface and zooming body is mounted on the clamp and eyepieces were inserted in the eyepiece sleeves. Camera was connected to the microscope by attaching it to the C mount cap provided on the microscope zooming body. Direction of the camera head was adjusted using the fixing screw and rotating the C mount. “Capture OEM version 2.3.7.9” is an image capture application software that was downloaded from pixelINK website. The camera connects to the computer via 3.5 W firewire cable.

The chip was fixed to a microscopic stage which contains a fiber optic cable attached to the light source. If needed, a flow resistor can be connected between the pump and microfluidic chip based on the desired flow rate and viscosity of fluid. Priming the system was important to make sure there was no air in the tubes by letting the fluids flow through the tubing for sufficient time till all the air is expelled. Once the system was primed, both pumps were connected to the chip using the FEP tubing. In the image capture application, under “video capture” tab, clicking on “play” provides the video feed from the camera. The position of chip, zoom and focus of microscope were adjusted to

get a sharp image of the X-junction on the screen. After the experiment was finished, the chips and flow channels were cleaned thoroughly by running isopropanol, water and air to remove any process liquid from the system.

3.2.2 Emulsion Formation

There is a power button provided on each pump to turn them on. The compressed air supply valve was turned on and flow rates of each fluid were entered in the FCC software. Flow rate/ pressure was adjusted until a steady stream of droplets was generated at the junction. Figure 11 shows the mechanism of droplet formation in the junction by shearing of the droplet phase fluid by the continuous phase fluid. In Figure 12, a continuous stream of droplets formed at the junction can be seen.

Following steps are to be followed in the “OEM application” to capture droplet images/videos:

For images: “Image capture” tab → “capture” → Check “increment file name after capture”

For videos: “Video capture” tab → “begin capture” → Check “increment file name after capture”

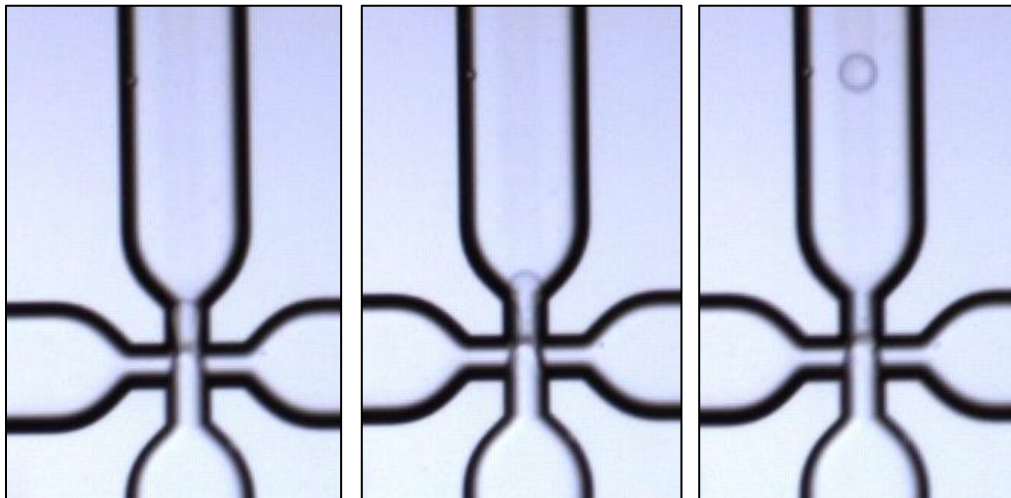


Figure 11: Shearing of the droplet phase fluid and droplet formation process

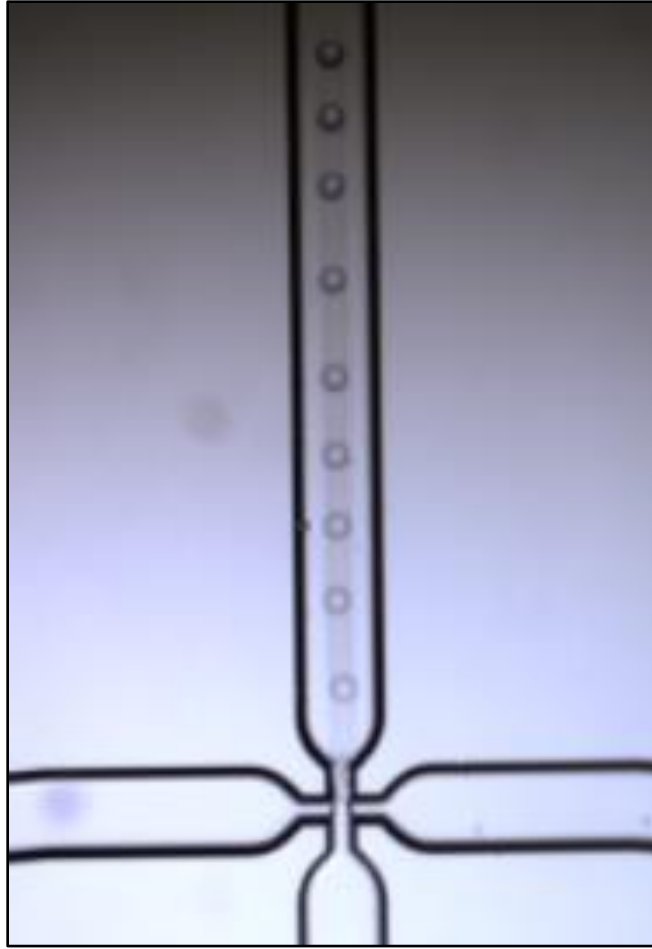


Figure 12: Continuous stream of n-decane droplets in water are formed at the X-junction of 100 μm hydrophilic chip; continuous phase flow rate = 150 $\mu\text{l}/\text{min}$, droplet phase flow rate = 1.25 $\mu\text{l}/\text{min}$

3.2.3 Emulsion Stability Analysis

For conducting the stability experiments, the emulsion created was carefully collected in a glass vial. After that it was observed under the microscope to find out the temporal evolution of droplet size, and coalescence rates.

3.3 Data Analysis

To measure droplet images μScope Professional version 21.1 was installed. It is an image analysis application supplied by PixeLINK. Snapshots of videos were captured and converted to appropriate format compatible with the software. These images were then uploaded on the image analysis

application. The width of channel was used as a reference for calibration. After measuring the droplet diameters, the data was exported to an excel file for further analysis. For each set of flow conditions, diameters were measured for 10 different droplets that are on different frames and the average size and standard deviation were calculated. Within the limits of measurement error, it can be said that the droplets are very monodispersed. Figure 13 shows the measurement of droplet diameter using μ Scope Professional software. It can be seen from the figure that the channel diameter which was known to be $300\ \mu\text{m}$ was used as the reference to measure droplet sizes.

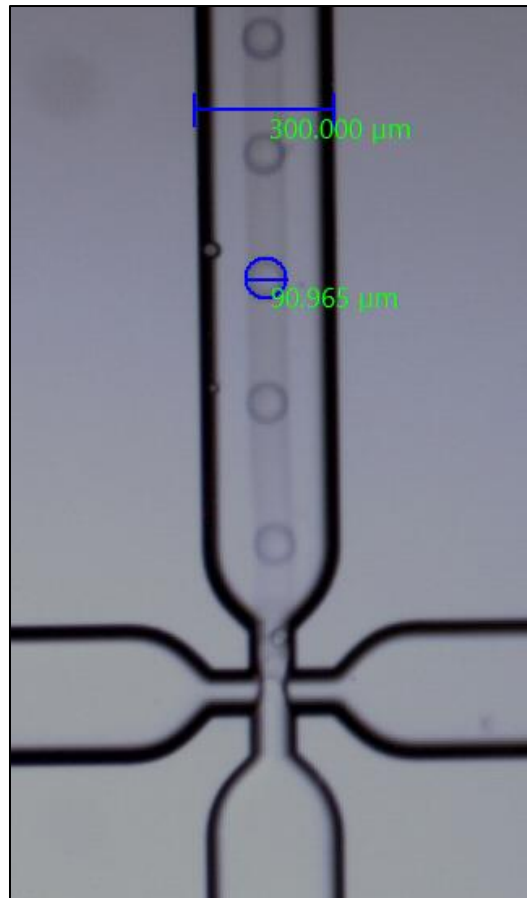


Figure 13: Droplet size measurement using μ Scope Professional using channel diameter as the reference dimension

CHAPTER IV

EXPERIMENTAL RESULTS

4.1 Effect of Various Parameters on Droplet Size

In the following sections, the effects of various process parameters on droplet size are discussed.

4.1.1 Oil and Water fraction/Flow rates

Figures 18-23 indicate that for a constant flow rate of the continuous phase fluid, the droplet diameters do not change significantly with water-cut (in a hydrophobic chip) or oil fraction (hydrophilic chip). It only changes the frequency of droplet formation. However, it is important to specify that the studied ranges of oil and water-cut are very narrow and less than 1% (i.e. dilute emulsions). As can be observed from the figures, both the water and oil droplet sizes are certainly a strong function of external phase flow rate and the droplet size decreases with an increase in external phase flow rate.

In figures 14 and 15, n-decane was used as the oil phase fluid while DI water was the aqueous phase fluid. When NaCl solution was used instead of DI water as the aqueous phase, similar trends of oil and water fraction effect on droplet diameter can be observed. In figures 16 and 17, 2.5% w/w NaCl solution in water was used as the aqueous phase. Similarly, 12.5% NaCl solution in water was used as aqueous phase fluid in figures 18 and 19. The effect of flow rates on the droplet size can also be seen from figures 14-19. The flow rates mentioned in the legend refer to the continuous phase flow rates. At a constant continuous phase flow rate, droplet diameter does not

change significantly with variation of droplet phase flow rate. However, increasing the continuous phase flow rate causes a decrease in droplet diameter in all the cases.

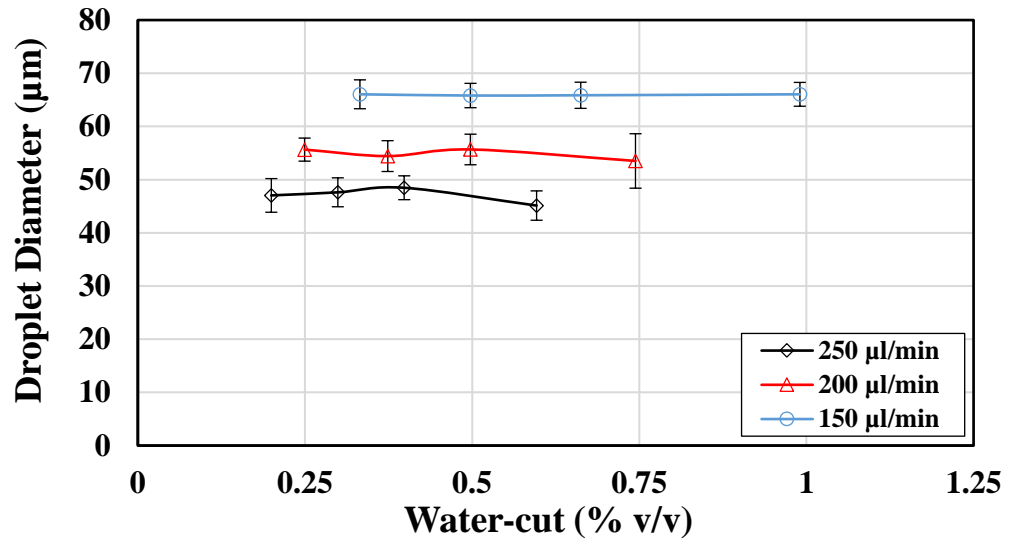


Figure 14: Effect of water-cut on water droplet size; aqueous phase: deionized water; organic phase: n-decane; 100 µm hydrophobic chip

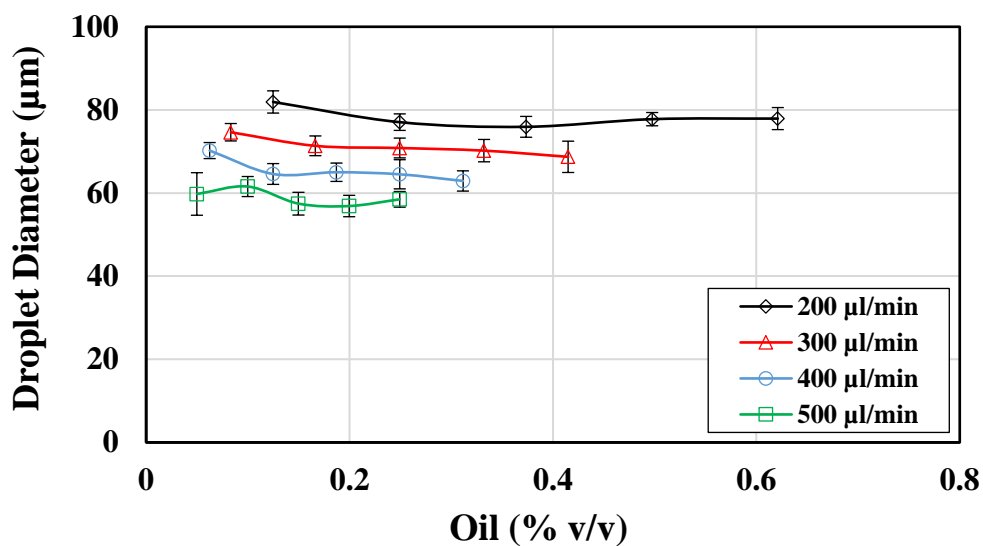


Figure 15: Effect of oil% on oil droplet size; aqueous phase: deionized water; organic phase: n-decane; 100 µm hydrophilic chip

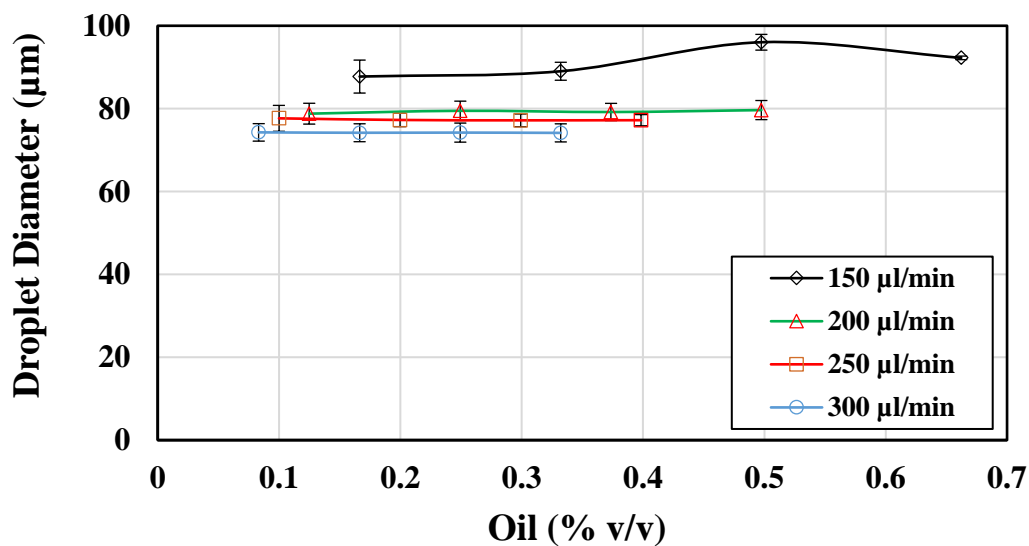


Figure 16: Effect of oil% on oil droplet size; aqueous phase: 2.5% w/w NaCl solution in water; organic phase: n-decane; 100 µm hydrophilic chip

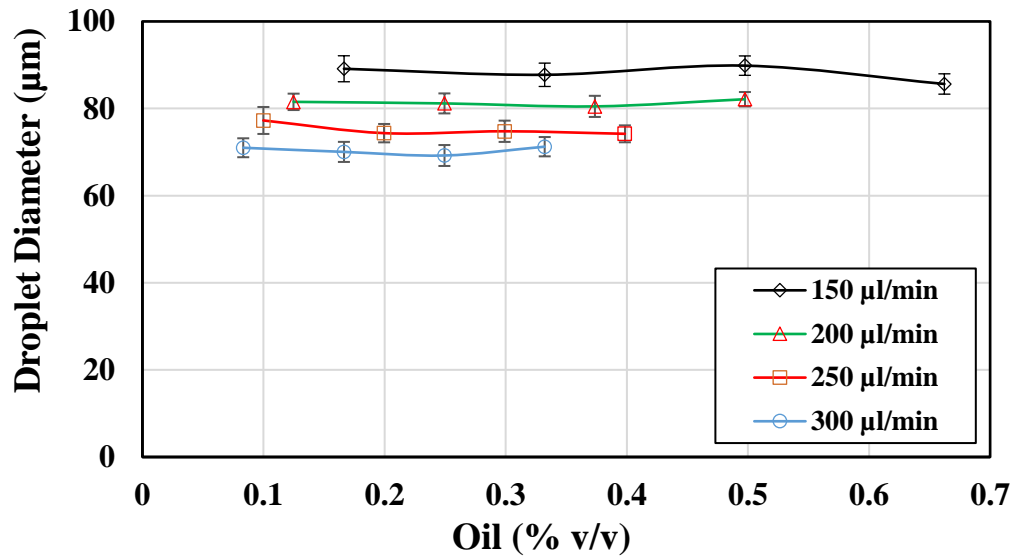


Figure 17: Effect of oil% on oil droplet size; aqueous phase: 12.5% w/w NaCl solution in water; organic phase: n-decane; 100 µm hydrophilic chip

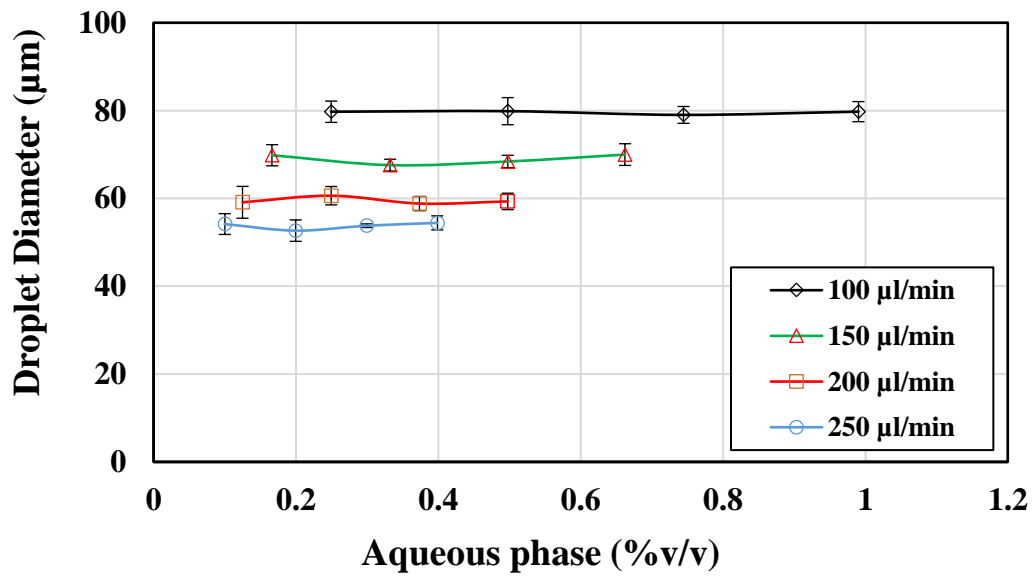


Figure 18: Effect of water-cut on water droplet size; aqueous phase: 2.5% w/w NaCl solution in water; organic phase: n-decane; 100 µm hydrophobic chip

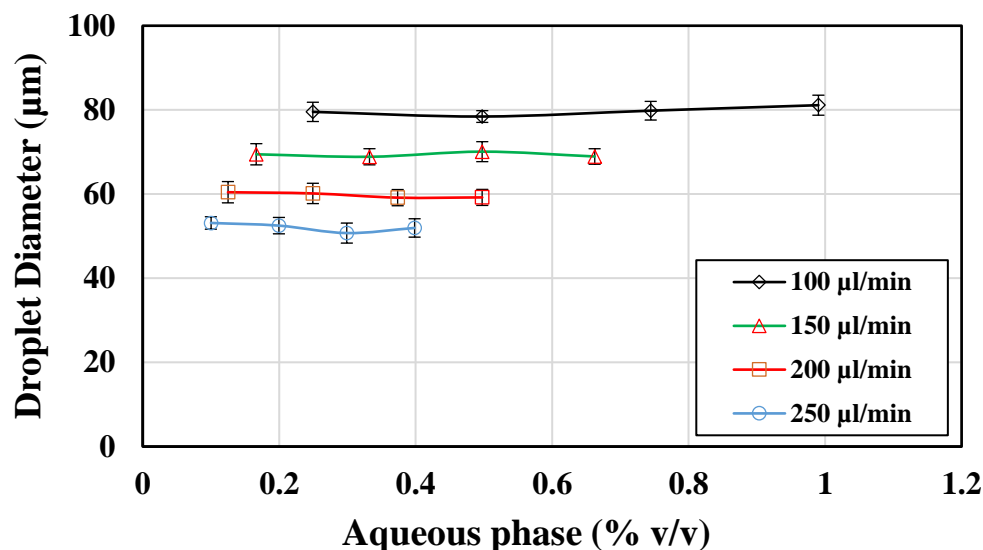


Figure 19: Effect of water-cut on water droplet size; aqueous phase: 12.5% w/w NaCl solution in water; organic phase: n-decane; 100 µm hydrophobic chip

4.1.2 Organic Phase

To compare the effect of organic phase fluid on droplet diameter, n-decane and n-hexadecane were used. DI water was used as the continuous phase fluid. As can be observed in figure 20, the diameter of n-decane droplets formed are slightly smaller than n-hexadecane droplets for same continuous and droplet phase flow conditions. It can be explained by the fact that higher viscosity of the droplet phase results in bigger droplets [44]. This is because at low viscosities, droplet break-up is governed by the rate-of-flow-controlled breakup suggesting that the volume of droplets is inversely proportional to continuous phase flow rate [44]. At high viscosities, a pressure buildup takes place as the neck between the emerging droplet and stream of droplet phase fluid is squeezed by the continuous phase. The droplet breakup takes larger time and droplets are larger [44]. Since the viscosity of n-hexadecane (3.059 at 25 °C) is higher than n-decane (0.849 at 25 °C), it is expected to form bigger droplets in a O/W emulsion [45, 46].

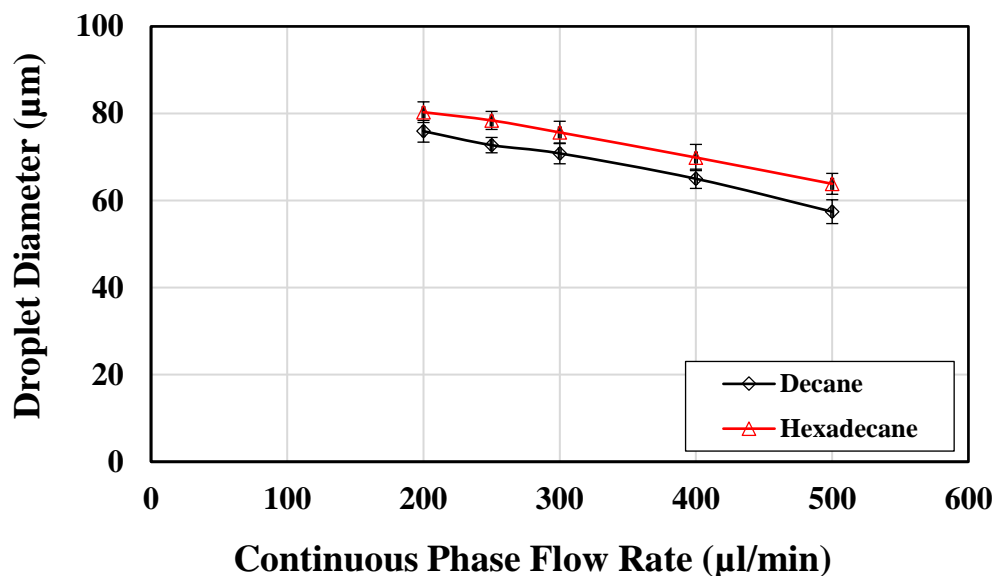


Figure 20: Effect of organic phase on oil droplet size; continuous phase: DI water; droplet phase flow rate = 0.75 µl/min; 100 µm hydrophilic chip

4.1.3 Salt Type and Concentration

For these experiments, n-decane was used as the oil phase and NaCl, KCl or CaCl₂ solutions were used as the aqueous phase fluids. It was observed that within the experimental uncertainty the type and concentration of these salts do not affect the droplet diameter during emulsion formation (Figure 21). 10 different droplet diameters were calculated at each salt concentration and average of these 10 diameters was used in the plot. For pure (0% salt concentration) fluids data, three different experiments were conducted and 10 droplets from each of them (total of 30 droplets) were used to calculate the average droplet diameter and standard deviation. It can be also seen from figure 21 that the oil droplets formed in O/W emulsion are larger than water droplets in a W/O emulsion.

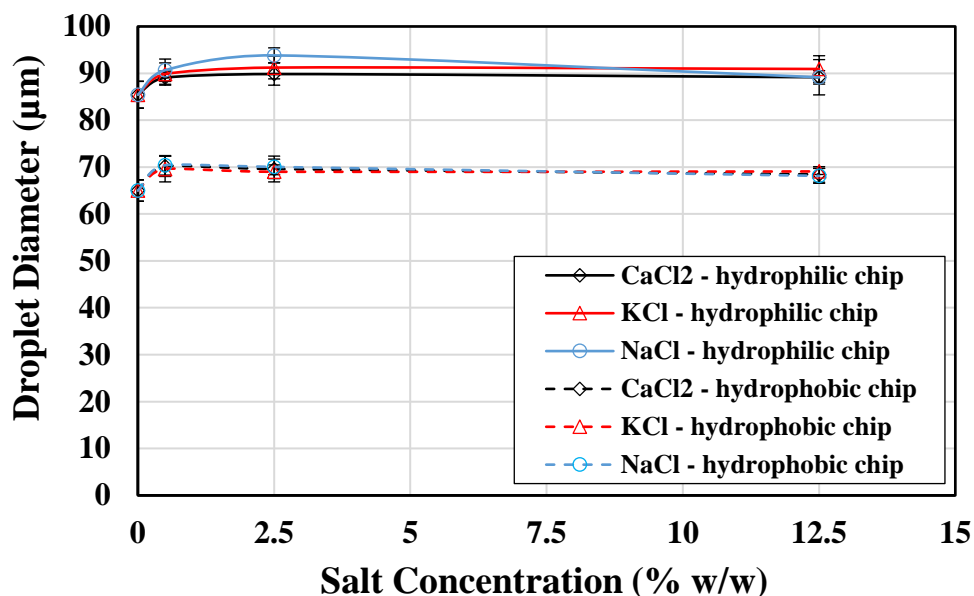


Figure 21: Effect of salt concentration and salt type on oil (in hydrophilic chip) and water (in hydrophobic chip) droplet size; droplet phase flow rate = 0.75 $\mu\text{l}/\text{min}$, continuous phase flow rate = 150 $\mu\text{l}/\text{min}$.

4.1.4 Surfactant Type and Concentration

Figures 22 and 23 demonstrate the effect of surfactant type (SDS and Span 80) and concentration on droplet size as well as repeatability runs for W/O emulsion using Span 80 as surfactant. SDS was used as a water soluble surfactant and Span 80 was an oil soluble surfactant. The CMC of SDS in water at 25 °C is 2.36 g/l [23]. Flow rate of continuous phase fluid was 150 $\mu\text{l}/\text{min}$ and that of droplet phase fluid was 0.75 $\mu\text{l}/\text{min}$. It can be seen from Figure 22 that the droplet size of both oil (hydrophilic chip) and water droplets (hydrophobic chip) decrease sharply up to the CMC value and after that there is a very gradual decline for a hydrophilic chip. Similar trend was observed when Span 80 is used as a surfactant (Figure 23). For these data points an average diameter of 20 droplets and the corresponding standard deviations are used.

Similar experiments were also conducted for a different set of flow conditions with continuous phase flow rate as 200 $\mu\text{l}/\text{min}$ and droplet phase flow rate as 0.75 $\mu\text{l}/\text{min}$. The trends obtained in

this case were identical to the previous conditions as can be seen from figure 24 (using SDS as surfactant) and figure 25 (using Span 80 as surfactant).

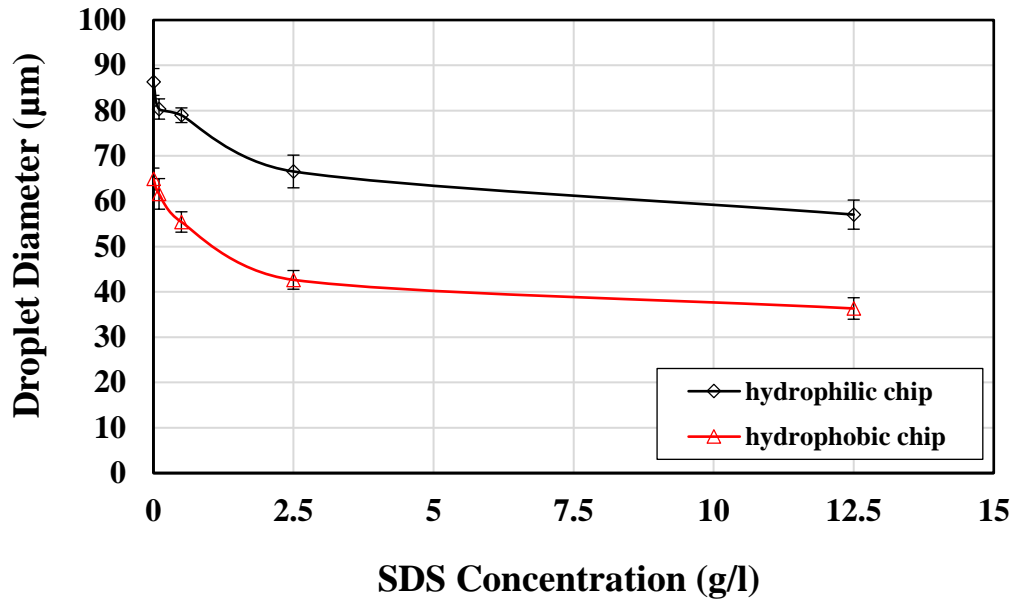


Figure 22: Effect of SDS concentration on oil and water droplet size, continuous phase flow rate = 150 $\mu\text{l}/\text{min}$, droplet phase flow rate = 0.75 $\mu\text{l}/\text{min}$; 100 μm chip

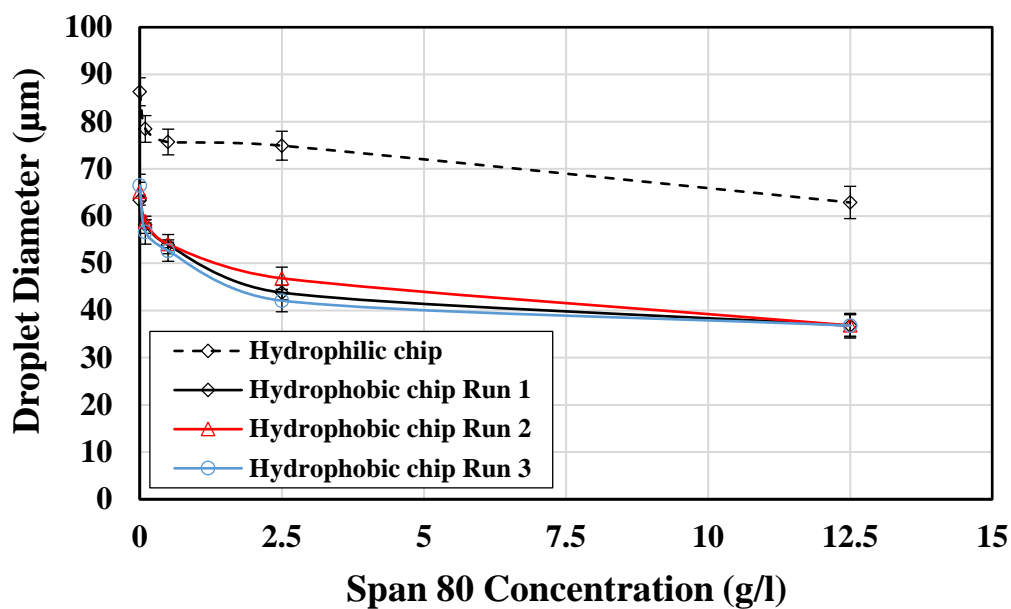


Figure 23: Effect of Span 80 concentration on oil and water droplet size, continuous phase flow rate = 150 $\mu\text{l}/\text{min}$, droplet phase flow rate = 0.75 $\mu\text{l}/\text{min}$; 100 μm chip

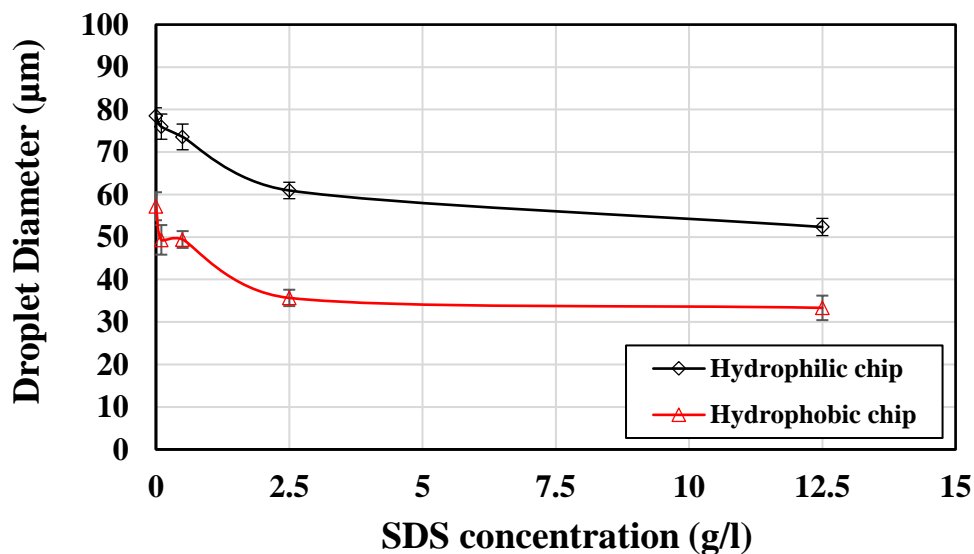


Figure 24: Effect of SDS concentration on oil and water droplet size, continuous phase flow rate = 200 $\mu\text{l}/\text{min}$, droplet phase flow rate = 0.75 $\mu\text{l}/\text{min}$; 100 μm chip

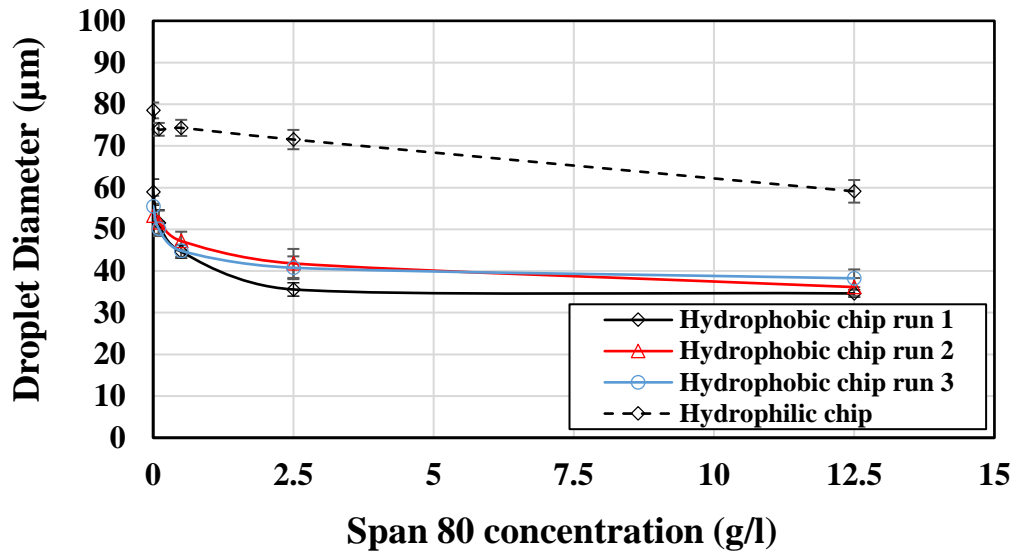


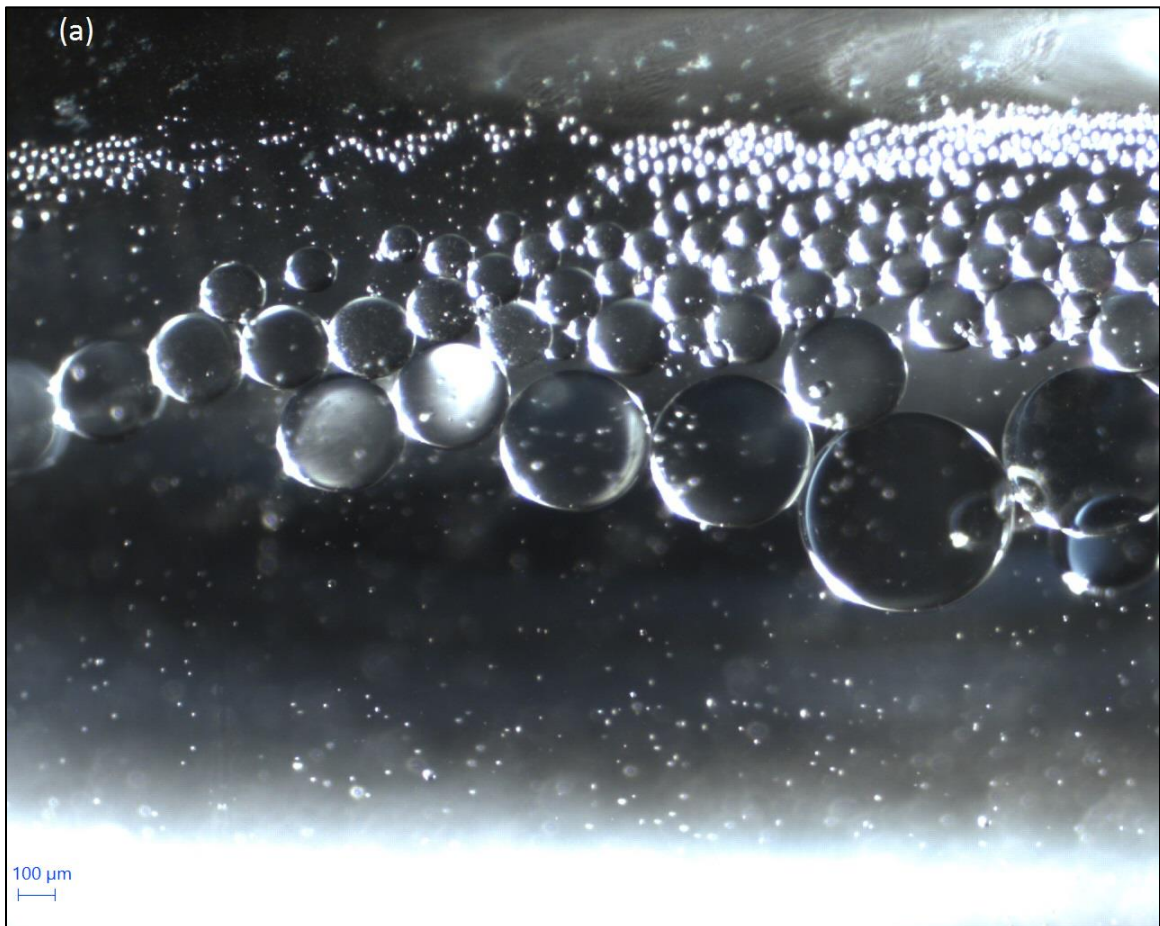
Figure 25: Effect of Span 80 concentration on oil and water droplet size, continuous phase flow rate = 200 $\mu\text{l}/\text{min}$, droplet phase flow rate = 0.75 $\mu\text{l}/\text{min}$; 100 μm chip

For repeatability runs, three different experiments were carried out in a hydrophobic chip using Span 80 as a surfactant and the average diameter of 10 droplets from each run was calculated and plotted along with the pure fluid (without any surfactant) data. As can be seen in figures 23 and 25, a very good repeatability was obtained among the runs. Although the droplets were highly monodispersed in all the other cases, small daughter droplets were formed at 12.5 g/l concentration of span 80 in n-decane using hydrophobic chip and the measured diameters were for the mother droplets.

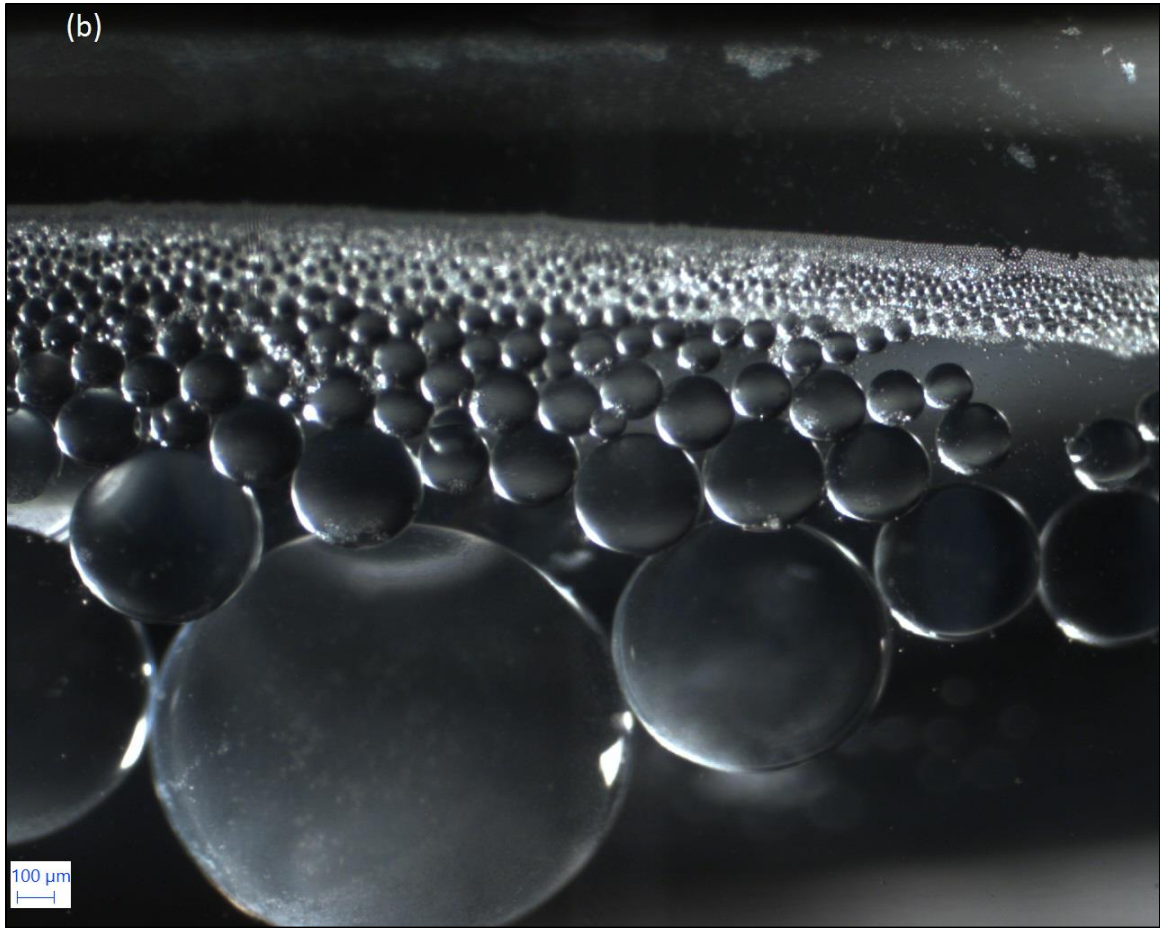
4.2 Stability Analysis

Stability experiments were carried out to observe droplet-droplet and droplet-interface coalescence phenomena. First of all, O/W droplets were produced using n-decane as the oil phase and DI water as the aqueous phase. In the subsequent experiments, either SDS or Span 80 were used as surfactant to compare the droplet sizes and coalescence rates with and without the presence of surfactants.

Figures 26 (a) and (b) indicate the presence of polydispersed droplets with a wide size distribution in the absence of a surfactant. In 26 (a), the picture was taken immediately after the formation of emulsions and collection in a vial while 26 (b) was taken after 8 hours. This is due to the coalescence of droplets inside the tubes. Droplets produced at the junction were monodispersed but the emulsion was unstable and coalescence of droplets was taking place leading to the formation of big droplets of the order of several hundreds of micrometers. Some air bubbles can also be seen at the top in figures 26 (a) and (b). The number of bubbles increased slowly over time as they reached the interface from the bulk of liquid.



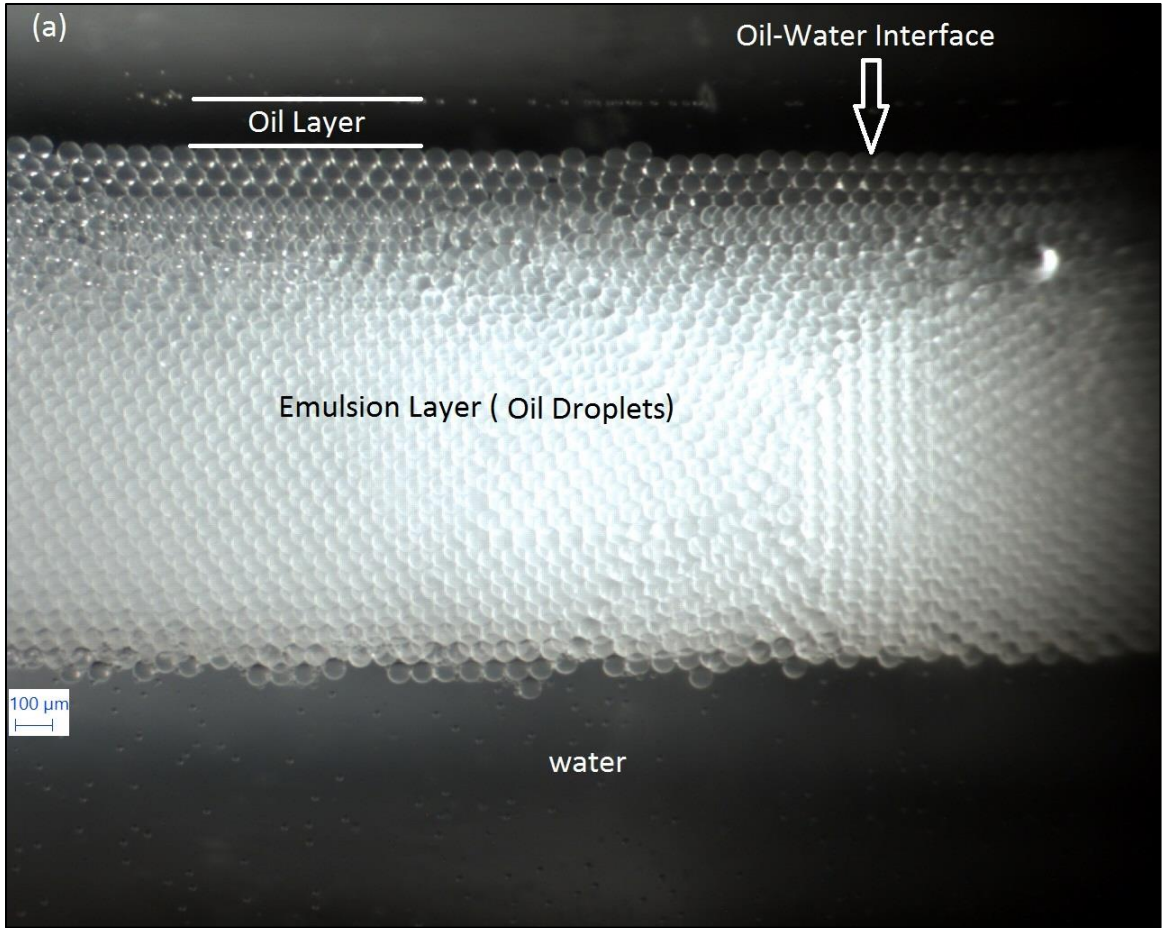
(a)



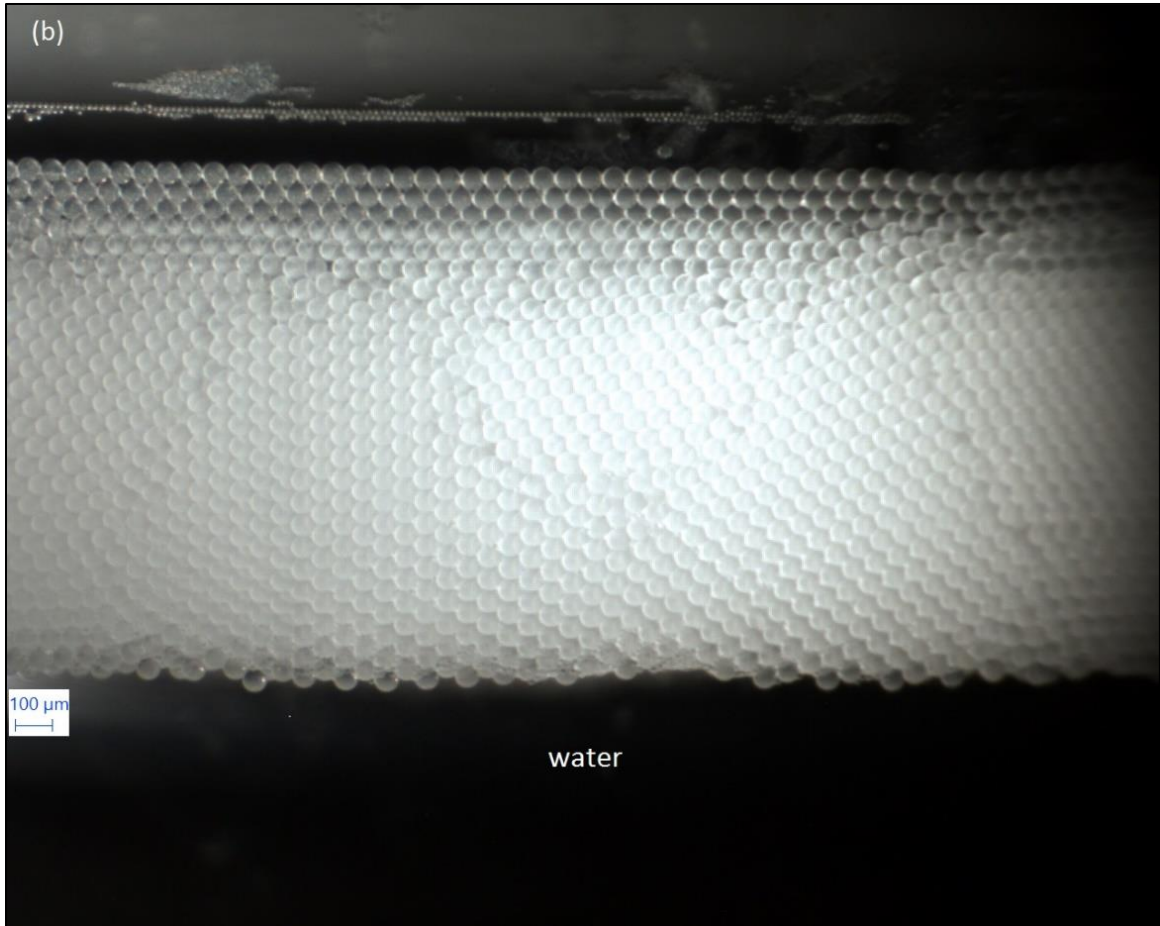
(b)

Figure 26: Stability analysis for O/W emulsion; aqueous phase: deionized water, oil phase: n-decane; (a) immediately after emulsion formation, (b) after 8 hours

A 2.5 g/l solution of Span 80 in n-decane was used to prepare O/W emulsion which was collected in a vial and the droplets were observed for coalescence phenomena. As it can be seen in the figure 27 (a), by the end of emulsion collection time the droplets were already sedimented and formed a dense packed zone at the water-oil interface. The emulsion was observed to be a Winsor type III which means free water and oil layers existed with a middle phase of microemulsion [47]. It can also be noticed in the figure 27 (b) that the emulsion is highly monodispersed and is very stable with no droplet-droplet or droplet-interface coalescence even after 8 hours.



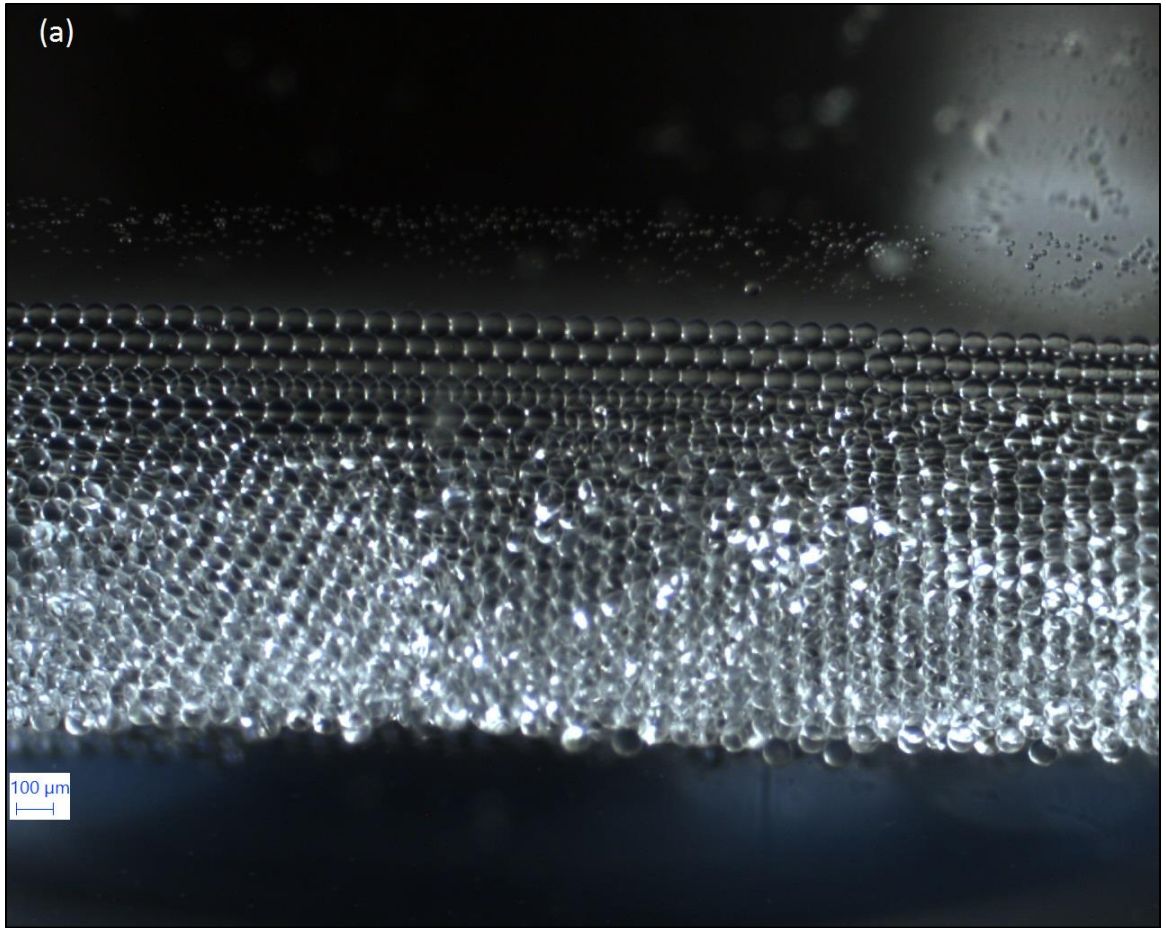
(a)



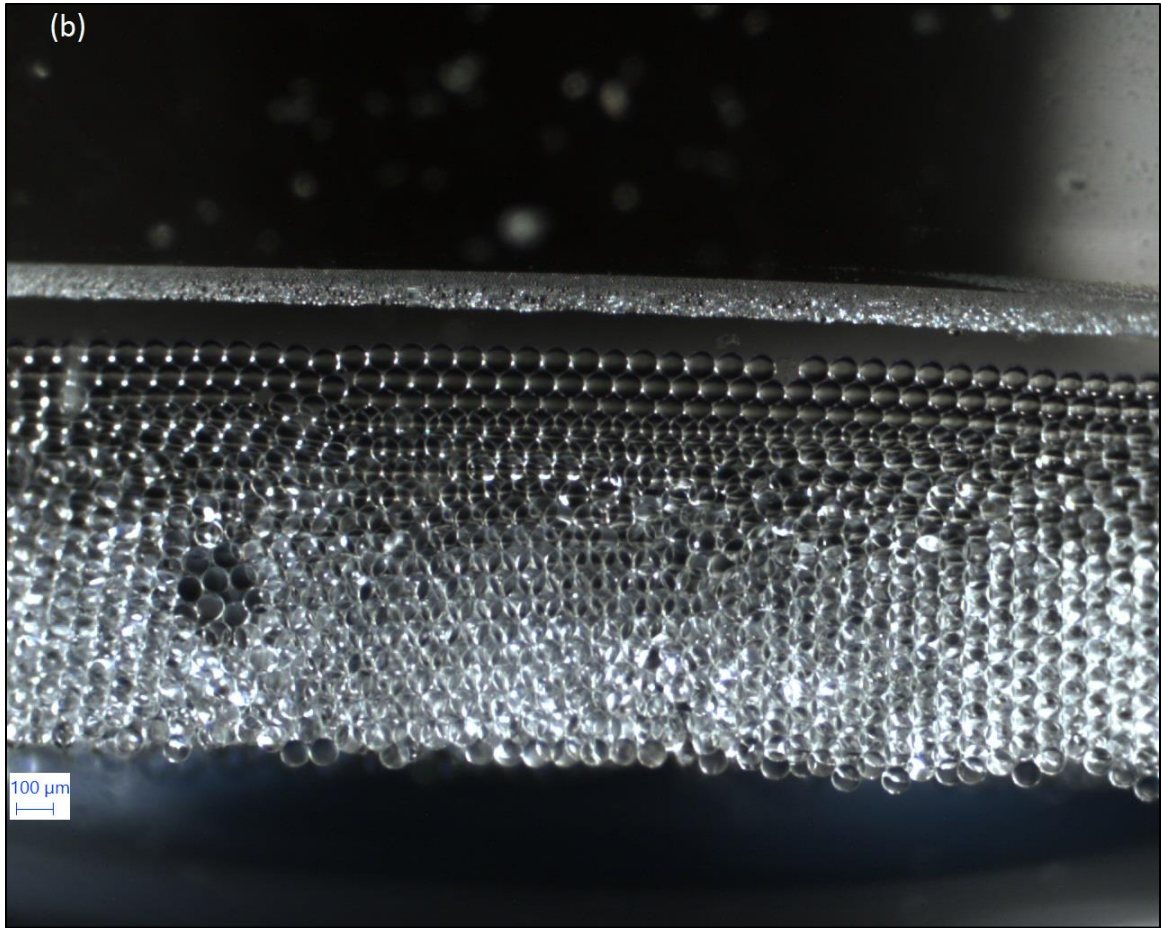
(b)

Figure 27: Stability analysis for O/W emulsion; aqueous phase: deionized water, oil phase: 2.5 g/l Span 80 solution in n-decane; (a) immediately after emulsion formation, (b) after 8 hours

Similar experiments were also carried out using SDS as a surfactant in the aqueous phase and monodispersed O/W droplets were generated in a hydrophilic chip. 0.5 g/l and 2.5 g/l solutions of SDS in water were used for two different experiments. Oil phase consisted of n-decane in both the cases.



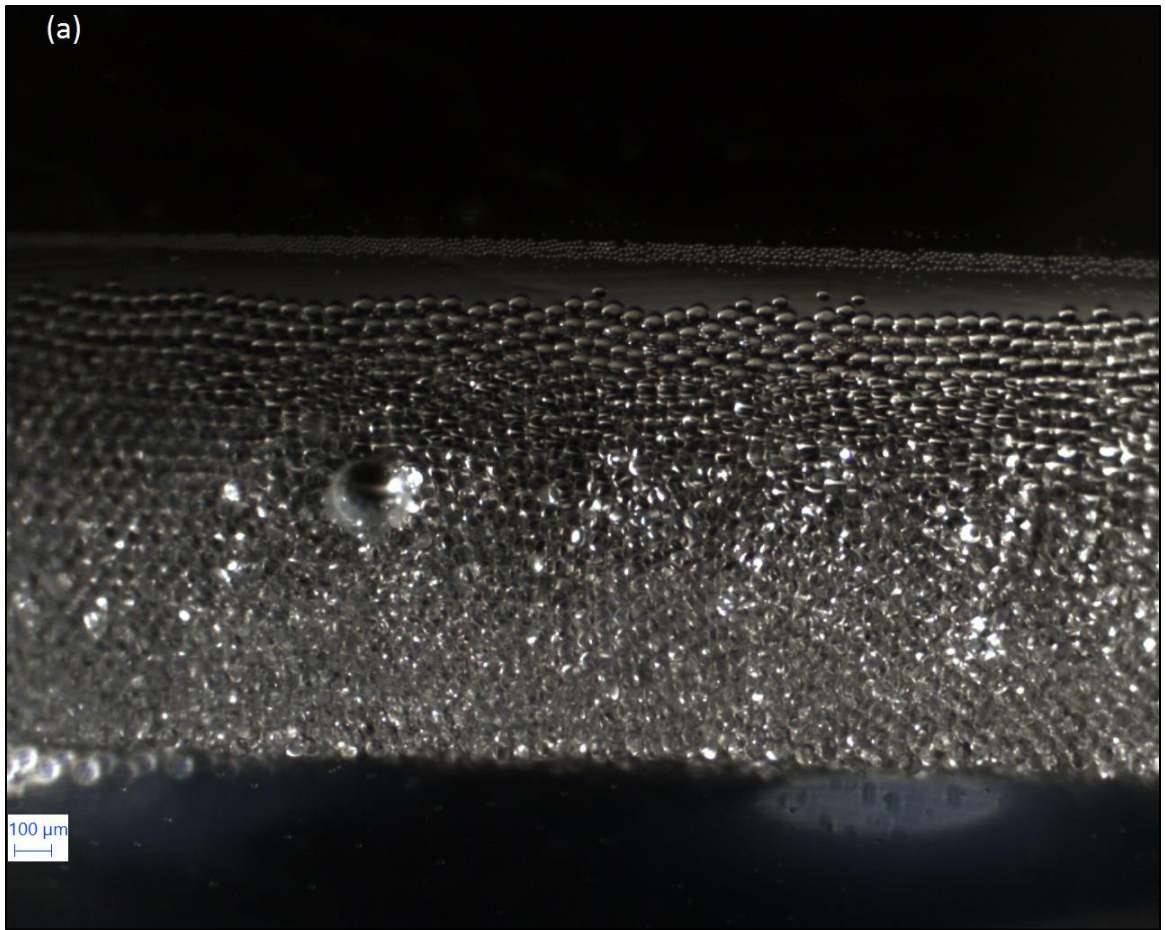
(a)



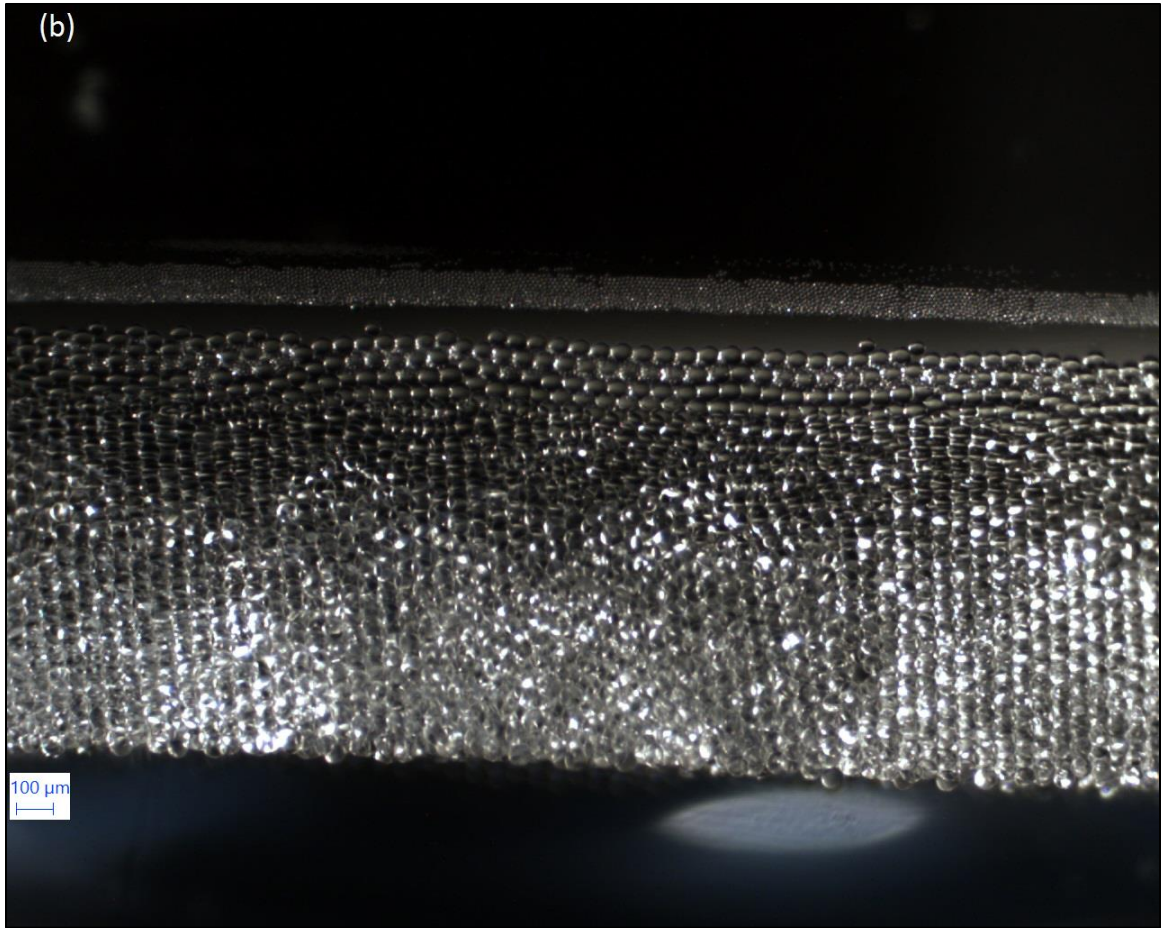
(b)

Figure 28: Stability analysis for O/W emulsion; aqueous phase: 0.5 g/l SDS solution in water, oil phase: n-decane; (a) immediately after emulsion formation, (b) after 8 hours

Figures 28 (a) and (b) shows the stability experiment for 0.5 g/l SDS solution. It can be seen that the emulsion was very stable and there is no droplet coalescence even after 8 hours.



(a)



(b)

Figure 29: Stability analysis for O/W emulsion; aqueous phase: 2.5 g/l SDS solution in water, oil phase: n-decane; (a) immediately after emulsion formation, (b) after 8 hours

Similarly, in Figures 29 (a) and (b) stability experiment has been carried out for 2.5 g/l SDS solution. In this case also no droplet coalescence was taking place and the emulsion was stable. The size of droplets was consistent with the measured droplet diameters during droplet generation.

CHAPTER V

DISCUSSIONS

5.1 Major Conclusions

The main idea for this research was to generate emulsions using a microfluidic facility and find out the effect of various process parameters on droplet diameter and hence, emulsion stability. Stability analysis was also carried by collecting the generated emulsions in a vial and by observing the temporal evolution of emulsions. Monodispersed O/W and W/O emulsions were successfully generated in a microfluidic chip using hydrophilic and hydrophobic chips respectively and the droplets diameters were measured. It was observed that the formation of monodispersed droplets takes place only in some specific flow rate combinations of the droplet and continuous phase fluids. For other flow rates either polydispersed droplets or no droplets were observed. Only those conditions where monodispersed droplets were formed have been reported in this thesis. The important conclusions that can be drawn from this research are given below.

Main conclusion from the experiments is that microfluidics can be successfully used for emulsion formation and characterization. The following conclusions can be drawn from the droplet characterization in the emulsions:

1. While salt type and concentration have negligible effect on the droplet diameter of emulsions, surfactants significantly reduced the size of droplets, characterized by a sharp decrease in diameter till the critical micelle concentration followed by gradual or almost no decrease in droplet size on further increase in surfactant concentration.

2. An increase in the flow rate of continuous phase fluid caused the droplet diameter to decrease. Whereas, within the experimental range and uncertainty it can be concluded that droplet phase flow rate has almost no effect on droplet diameter at low concentrations of dispersed phase.
3. The change in water-cut has no effect on the size of water droplets in a W/O emulsion. Similarly, oil% had no effect on oil droplet size in O/W emulsion within the limits of experimental uncertainty.
4. The size of oil droplets formed in a hydrophilic chip are much larger (approx. 25-30 μm) than the water droplets produced in a hydrophobic chip.
5. N-decane forms smaller droplets compared to n-hexadecane in a hydrophilic chip probably due to lower viscosity of n-decane and ease of shearing of droplet.

Major conclusions from the stability experiment are:

1. In the absence of any surfactant the O/W emulsion consisting of n-decane droplets in a continuous water phase, show a droplet size distribution and the size of average droplet is much larger than that observed at the generation point. This indicates that the emulsion is unstable and droplets tend to coalesce while traveling through the tubes before reaching the collection vial.
2. Stable monodispersed emulsions were formed without any droplet coalescence when surfactants were used either in aqueous or organic phase. There were no droplet-droplet and droplet-interface coalescence even after several hours of standing in the vial.

5.2 Future Work

There is a scope for far more research in microfluidics based emulsion studies. One possibility is to establish the dripping, jetting and transition regimes encountered in a microfluidic device and find out the flow conditions resulting in monodispersed and polydispersed emulsions. Custom made chips can be used to produce multiple emulsions i.e. O/W/O and W/O/W finding applications

beyond the oil and gas industry. Reynolds number can be calculated for the flow conditions in this research and Darcy's equation for flow through porous media can be used to validate the experimental results.

Modeling of these emulsions can also be carried out using certain simulation softwares like Ansys Fluent and certain specialized softwares like Microfluidic module in Comsol. The choice of model to solve the flow equations depend on a number of factors ranging from the concentration of dispersed phase, laminar/turbulent flow and whether there is a significant change in temperature of the system. Complicated systems like these require large computation times in order to get high accuracy and often a compromise has to be made in order to get optimum results in least possible time and reasonable accuracy. Apart from this, it is also possible to carry out statistical analysis of the data.

REFERENCES

1. Larsson, K. and S.E. Friberg, *Food emulsions*. 1990: Marcel Dekker Inc.
2. Onuki, Y., et al., *MRI as a promising tool for evaluation of the stability of cosmetic emulsions*. International journal of cosmetic science, 2015.
3. Onuki, Y., et al., *Self-organizing Map Analysis for Understanding Comprehensive Relationships between Formulation Variables, State of Water, and the Physical Stability of Pharmaceutical Emulsions*. Chemical and Pharmaceutical Bulletin, 2015. **63**(11): p. 901-906.
4. Lim, J., et al., *A review on the effects of emulsions on flow behaviours and common factors affecting the stability of emulsions*. Journal of Applied Sciences, 2015. **15**(2): p. 167.
5. Kokal, S.L., *Crude oil emulsions: A state-of-the-art review*. SPE Production & facilities, 2005. **20**(01): p. 5-13.
6. Manz, A., N. Graber, and H.á. Widmer, *Miniaturized total chemical analysis systems: a novel concept for chemical sensing*. Sensors and actuators B: Chemical, 1990. **1**(1): p. 244-248.
7. Inglis, D., *Microfluidic devices for cell separation*. 2007: Princeton University.
8. Stone, H.A., A.D. Stroock, and A. Ajdari, *Engineering flows in small devices: microfluidics toward a lab-on-a-chip*. Annu. Rev. Fluid Mech., 2004. **36**: p. 381-411.
9. Garstecki, P., H.A. Stone, and G.M. Whitesides, *Mechanism for flow-rate controlled breakup in confined geometries: A route to monodisperse emulsions*. Physical Review Letters, 2005. **94**(16): p. 164501.
10. Dupas, A., et al., *Mechanical degradation onset of polyethylene oxide used as a hydrosoluble model polymer for enhanced oil recovery*. Oil & Gas Science and Technology–Revue d'IFP Energies nouvelles, 2012. **67**(6): p. 931-940.
11. He, K., et al. *Validating surfactant performance in the eagle ford shale: A correlation between the reservoir-on-a-chip approach and enhanced well productivity*. in *SPE Improved oil recovery symposium*. 2014. Society of Petroleum Engineers.

12. Xu, K., et al., *Microfluidic Investigation of Nanoparticles' Role in Mobilizing Trapped Oil Droplets in Porous Media*. Langmuir, 2015. **31**(51): p. 13673-13679.
13. Conn, C.A., et al., *Visualizing oil displacement with foam in a microfluidic device with permeability contrast*. Lab on a Chip, 2014. **14**(20): p. 3968-3977.
14. Armstrong, R.T. and D. Wildenschild, *Investigating the pore-scale mechanisms of microbial enhanced oil recovery*. Journal of Petroleum Science and Engineering, 2012. **94**: p. 155-164.
15. Dong, M., Q. Liu, and A. Li, *Displacement mechanisms of enhanced heavy oil recovery by alkaline flooding in a micromodel*. Particuology, 2012. **10**(3): p. 298-305.
16. Lifton, V.A., *Microfluidics: an enabling screening technology for enhanced oil recovery (EOR)*. Lab on a Chip, 2016. **16**(10): p. 1777-1796.
17. Nic, M., et al., *IUPAC Compendium of Chemical Terminology-The Gold Book*. 2005: International Union of Pure and Applied Chemistry.
18. Sherman, P., *Emulsion science*. 1968: Academic Press.
19. McClements, D.J., *Food emulsions: principles, practices, and techniques*. 2015: CRC press.
20. Ogawa, S., E.A. Decker, and D.J. McClements, *Production and characterization of O/W emulsions containing droplets stabilized by lecithin-chitosan-pectin multilayered membranes*. Journal of agricultural and food chemistry, 2004. **52**(11): p. 3595-3600.
21. Anton, N., et al., *Nano-emulsions and nanocapsules by the PIT method: an investigation on the role of the temperature cycling on the emulsion phase inversion*. International Journal of Pharmaceutics, 2007. **344**(1): p. 44-52.
22. Solans, C., et al., *Nano-emulsions*. Current opinion in colloid & interface science, 2005. **10**(3): p. 102-110.
23. Pichot, R., *Stability and characterisation of emulsions in the presence of colloidal particles and surfactants*. 2010, The University of Birmingham.
24. Walstra, P., *Principles of emulsion formation*. Chemical Engineering Science, 1993. **48**(2): p. 333-349.
25. Christopher, G., et al., *Coalescence and splitting of confined droplets at microfluidic junctions*. Lab on a Chip, 2009. **9**(8): p. 1102-1109.
26. Rosen, M.J. and J.T. Kunjappu, *Surfactants and interfacial phenomena*. 2012: John Wiley & Sons.
27. Farn, R.J., *Chemistry and technology of surfactants*. 2008: John Wiley & Sons.

28. Scholz, E., *Karl Fischer titration: determination of water*. 2012: Springer Science & Business Media.
29. Fortuny, M., et al., *Effect of salinity, temperature, water content, and pH on the microwave demulsification of crude oil emulsions*. *Energy & Fuels*, 2007. **21**(3): p. 1358-1364.
30. McClements, D. and J. Coupland, *Theory of droplet size distribution measurements in emulsions using ultrasonic spectroscopy*. *Colloids and Surfaces A: Physicochemical and Engineering Aspects*, 1996. **117**(1): p. 161-170.
31. Sjöblom, J., et al., *Water-in-crude oil emulsions. Formation, characterization, and destabilization*, in *Surfactants and Macromolecules: Self-Assembly at Interfaces and in Bulk*. 1990, Springer. p. 131-139.
32. Khatib, Z., G. Hirasaki, and A. Falls, *Effects of capillary pressure on coalescence and phase mobilities in foams flowing through porous media*. *SPE reservoir engineering*, 1988. **3**(03): p. 919-926.
33. Wardlaw, N.C. and R. Taylor, *Mercury capillary pressure curves and the interpretation of pore structure and capillary behaviour in reservoir rocks*. *Bulletin of Canadian Petroleum Geology*, 1976. **24**(2): p. 225-262.
34. Levine, S., B.D. Bowen, and S.J. Partridge, *Stabilization of emulsions by fine particles II. capillary and van der Waals forces between particles*. *Colloids and surfaces*, 1989. **38**(2): p. 345-364.
35. Cassie, A. and S. Baxter, *Wettability of porous surfaces*. *Transactions of the Faraday Society*, 1944. **40**: p. 546-551.
36. Whitesides, G.M., *The origins and the future of microfluidics*. *Nature*, 2006. **442**(7101): p. 368-373.
37. Lin, C.-H., et al., *A fast prototyping process for fabrication of microfluidic systems on soda-lime glass*. *Journal of Micromechanics and Microengineering*, 2001. **11**(6): p. 726.
38. Ren, K., J. Zhou, and H. Wu, *Materials for microfluidic chip fabrication*. *Accounts of chemical research*, 2013. **46**(11): p. 2396-2406.
39. Skurtys, O. and J. Aguilera, *Applications of microfluidic devices in food engineering*. *Food Biophysics*, 2008. **3**(1): p. 1-15.
40. Song, H., D.L. Chen, and R.F. Ismagilov, *Reactions in droplets in microfluidic channels*. *Angewandte chemie international edition*, 2006. **45**(44): p. 7336-7356.

41. Sjöblom, J., et al., *Our current understanding of water-in-crude oil emulsions.: Recent characterization techniques and high pressure performance*. Advances in Colloid and Interface Science, 2003. **100**: p. 399-473.
42. Marmottant, P. and J.-P. Raven, *Microfluidics with foams*. Soft Matter, 2009. **5**(18): p. 3385-3388.
43. Krebs, T., C. Schroën, and R. Boom, *Coalescence kinetics of oil-in-water emulsions studied with microfluidics*. Fuel, 2013. **106**: p. 327-334.
44. Nie, Z., et al., *Emulsification in a microfluidic flow-focusing device: effect of the viscosities of the liquids*. Microfluidics and Nanofluidics, 2008. **5**(5): p. 585-594.
45. Hardy, R.C., *Viscosity of n-Hexadecane*. Journal of Research of the National Bureau of Standards, 1958. **61**(5): p. 433.
46. Dymond, J., *Viscosity of selected liquid n-alkanes*. Journal of physical and chemical reference data, 1994. **23**(1): p. 41-53.
47. Salager, J., et al., *Surfactant-oil-water systems near the affinity inversion part I: relationship between equilibrium phase behavior and emulsion type and stability*. JOURNAL OF DISPERSION SCIENCE AND TECHNOLOGY, 1982. **3**(3): p. 279-292.

VITA

Subarna Kole

Candidate for the Degree of

Master of Science

Thesis: APPLICATION OF MICROFLUIDICS FOR EMULSION
CHARACTERIZATION

Major Field: Chemical Engineering

Biographical:

Subarna Kole was born in Arambagh, India and grew up in Kanpur, India.

Education:

Completed the requirements for the Master of Science in Chemical Engineering at Oklahoma State University, Stillwater, Oklahoma in July, 2016.

Completed the requirements for the Bachelor of Science in Chemical Engineering at National Institute of Technology, Raipur, India in 2014.

Experience:

Worked as Graduate Research Assistant in the department of Chemical Engineering at Oklahoma State University, Stillwater from August 2014 to July 2016

Professional Memberships:

Student member of AIChE
Student member of SPE